Memristor for bio-inspired computing:

nonlinear circuits and mathematical models

Fernando CORINTO

fernando.corinto@polito.it

Politecnico di Torino (Italy)

Outline

- Motivation

- Memristor modeling and nonlinear dynamics
  - Model comparison
  - Influence on initial conditions
  - the SIMPLEST (passive) memristor circuit

- Conclusions

DATE workshop: Dresden, March 28, 2014
4th Memristor Symposium, ND (USA), July 28, 2014

Neuromorphic circuits

- The **Human Brain Project** in EU plans to use a supercomputer to recreate everything known about the human brain — a hugely ambitious goal!
- Leading neuroscientists in the US are now focussed on understanding how the brain works through the **Brain Activity Map** (BAM) project, but it's difficult to peer deeply enough into a brain to map the activity of every neuron. Because zebrafish embryos are transparent, the task is easier.
- Understand how neurons that make up the brain carry out their functions.

Neuromorphic circuits

MIT Technology Review

So the race is on to develop a different kind of chip that more accurately mimics the way the brain works. So-called **neuromorphic chips must be built from devices that behave like neurons** – in other words they transmit and respond to information sent in spikes rather than in a continously varying voltage.

One reason the brain is so **power efficient** is that neural spikes charge only a small fraction of a neuron as they travel. By contrast, conventional chips keep each and every transmission line at a certain voltage all the time.

Clearly, recent advancements in **memristor technology** and **spintronics** are making possible entirely new ways to design chips. However, **there is a long way to go** before synthetic systems can begin to match the capability of natural ones.

Beyond Moore's Law

INVITED PAPER
Proceedings of the IEEE | Vol. 100, May 13th, 2012

Science and Engineering Beyond Moore's Law

Device	Entity	Properties		
		Control Variable	State Variable	Output Variable
FET – Novel Materials (III-V, Ge, carbon-based, etc.)	Electron	Charge	Charge	Charge
SpinFET	Electron	Charge	Spin	Charge
Spin-Torque	Electron	Spin	Spin	Charge
Spin-Wave	Electron	Spin Waves	Spin	Charge Photon
Tunneling Transistor	Electron	Charge	Charge	Charge
Molecular switch	Electron or Atoms	Charge	Charge	Charge
NEMS	Atoms	Charge	Position	Charge
Atomic Switch	Atoms	Charge	Position	Electron
Memristor	Atoms	Charge	Charge,	Electron
Magnetic Cellular Automata	FM Domain	Magnetic dipole	Spin	FM Domain
Moving Domain Wall	FM Domain	Magnetic Dipole	Spin	FM Domain
Multi-Ferroic Tunnel Junction	FM Domain	Spin	Charge	Electron
Optical or Plasmonics	Atoms or Electrons	Charge	Optical Density	Photons
Thermal Transistor	Phonons	Thermal Energy	Temperature	Phonons

Taxonomy for Candidate Information Processing Devices

Breakthrough in Memristor

- **non-volatile memories → low–power, high–density**
- **neuromorphic systems → Memristor mimics biological synapse**
  - As in a living creature the weight of a synapse is adapted by the ionic flow through it, so the conductance of a memristor is adjusted by the flux across or the charge through it depending on its controlling source.
- **novel computer architectures → memory and process coexist**
  - Memristor will play a fundamental role in the realization of novel neuromorphic computing architectures merging memory and computation. This fundamental step will begin to bridge the main divide between biological computation and traditional computation, because memristor permits to bring data close to computation (the way biological systems do) and they use very little power to store that information.

Fundamentals of memristor

- non-volatile memories $\rightarrow$ low-power, high-density
- neuromorphic systems $\rightarrow$ memristors mimics synapses
- computer architectures $\rightarrow$ memory and processing coexist

Important issues:

- full understanding of nonlinear dynamics
- modeling

Memristor modeling
and
Nonlinear dynamics

What is a MEMRISTOR?

Memristor (L. O. Chua, 1971)


IEEE TRANSACTIONS ON CIRCUIT THEORY, VOL. CT-18, NO. 5, SEPTEMBER 1971

Memristor—The Missing Circuit Element

LEON O. CHUA, SENIOR MEMBER, IEEE

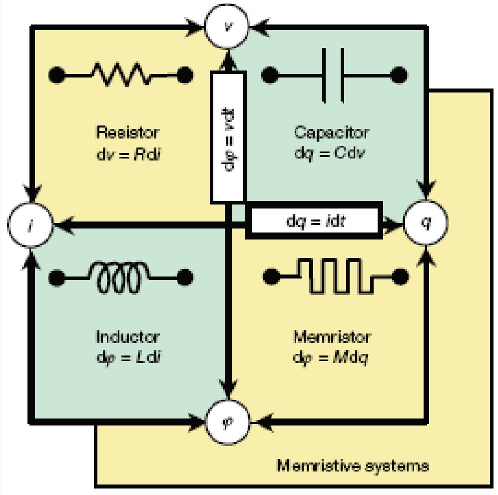

$$f_R(v(t), i(t)) = 0$$
$$f_C(v(t), q(t)) = 0$$
$$f_L(\varphi(t), i(t)) = 0$$
$$f_M(\varphi(t), q(t)) = 0$$

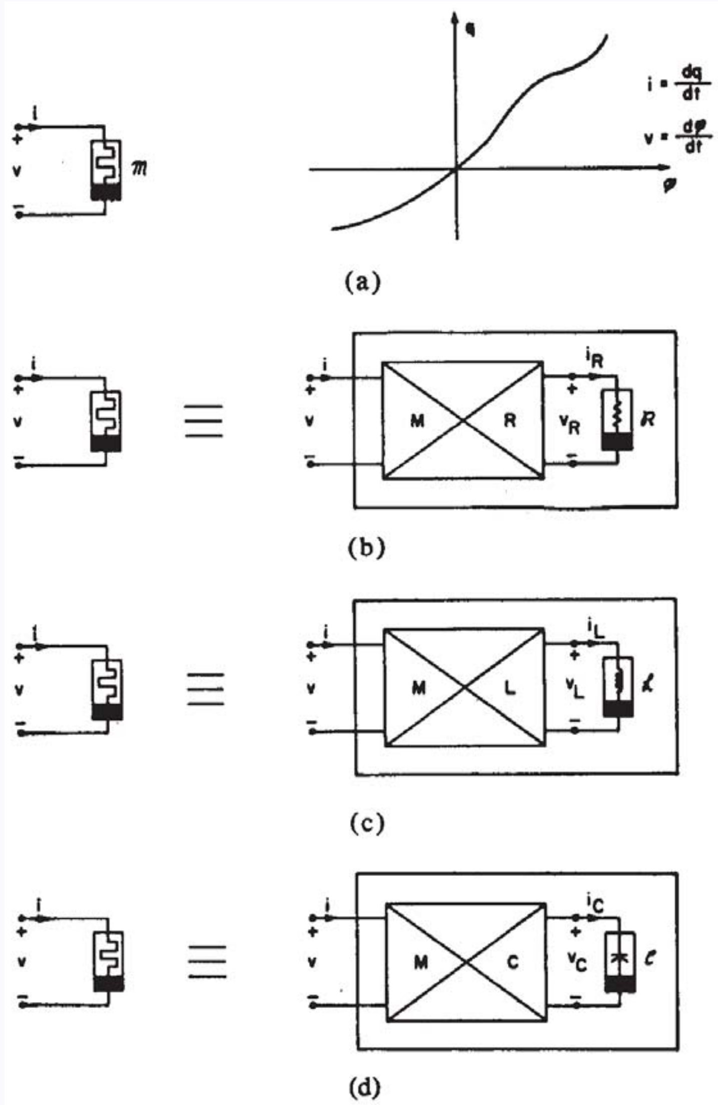

Charge-controlled "ideal" memristor

$$\varphi(t) = f(q(t)) \Rightarrow v(t) = M(q(t))\, i(t)$$

(memristance) $M(q(t)) = \dfrac{d\, f(q)}{dq}$

General memristive one-port (Chua and Kang, 1976)

$$v(t) = M(\mathbf{w}(t))\, i(t), \quad \mathbf{w} \in R^n$$

$$\frac{d\,\mathbf{w}(t)}{dt} = h(\mathbf{w}(t), i(t), t)$$

Recently, “Memristors” and “Memristive Devices” have been used interchangeably

Main properties:

- ☑ passivity criterion $\Rightarrow M(\mathbf{w}(t)) \geq 0$
- ☑ non-volatile memory property $\Rightarrow h(\mathbf{w}(t), 0, t) = 0, \quad \forall t$
- ☑ v-i pinched hysteresis loop (Lissajous figure) for any periodic source. The pinched hysteresis loop shrinks continuously as the frequency increases

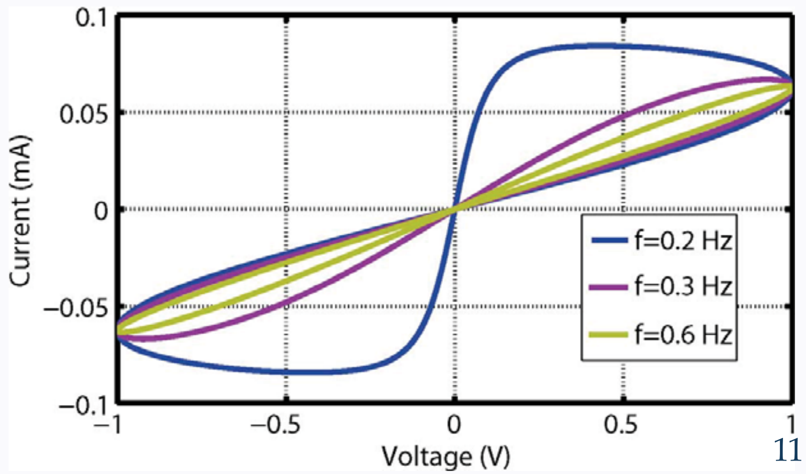

General memristive one-port (Chua and Kang, 1976)

Identical zero-crossing property

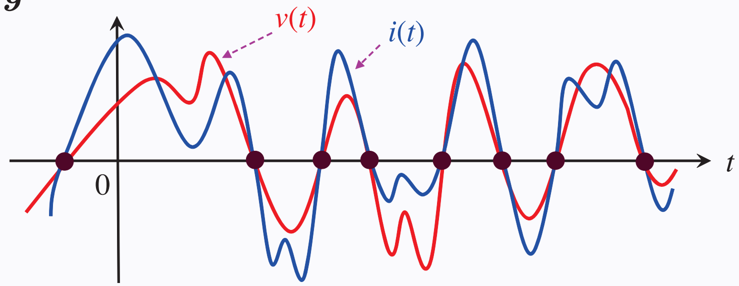

Fig. 5. Both $v(t)$ and $i(t)$ of a memristor with $0 < R(\mathbf{x}) < \infty$ and $0 < G(\mathbf{x}) < \infty$ must have identical zero crossings.

Frequency-dependent pinched hysteresis loop property

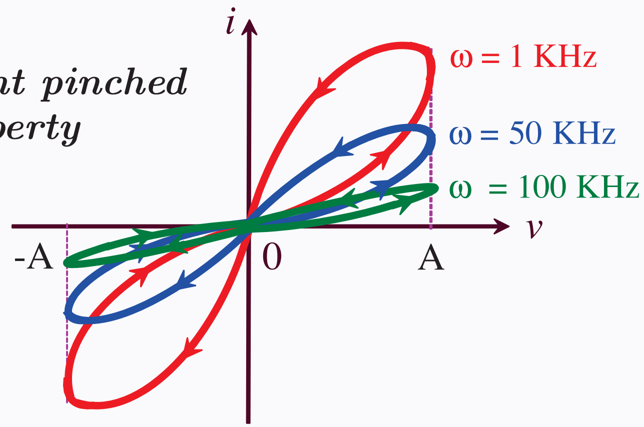

Fig. 7. Memristor *pinched hysteresis loop* shrinks continuously as the frequency ω increases. It tends to a straight line through the origin as $\omega \to \infty$.

Pinched hysteresis loop fingerprint

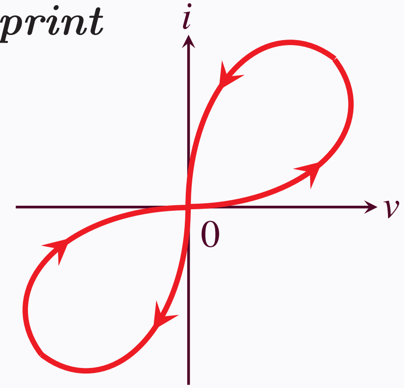

Example of a memristor pinched *hysteresis loop*.

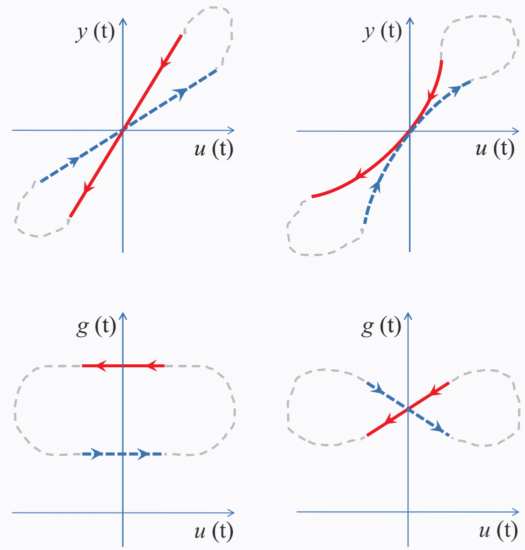

Yuriy V. Pershin[a]; Massimiliano Di Ventra[b]

HP Memristor (S. Williams et al, 2008)

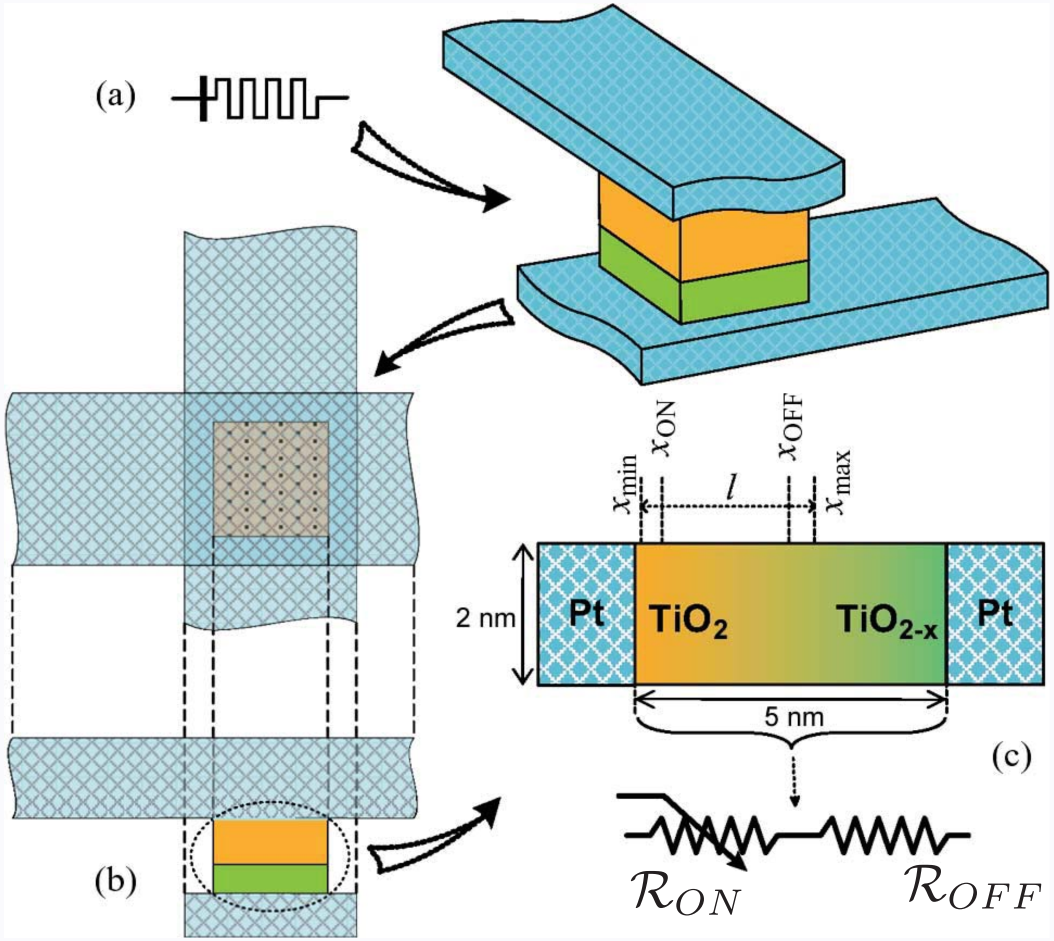

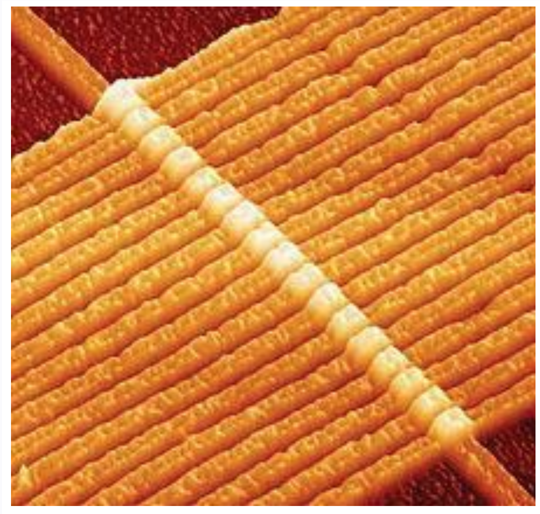

$$v(t) = \left(\mathcal{R}_{\mathrm{ON}} \frac{w(t)}{D} + \mathcal{R}_{\mathrm{OFF}}\left(1 - \frac{w(t)}{D}\right)\right) i(t)$$

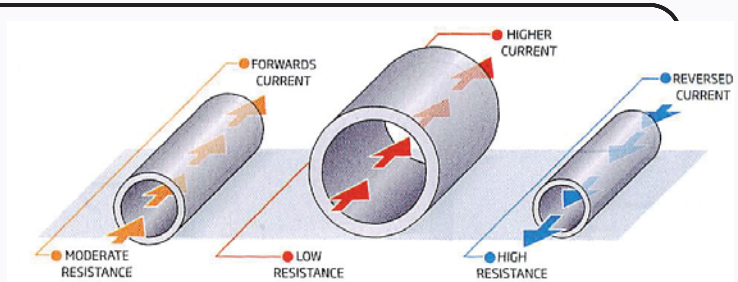

Mappings:

- water $\Longleftrightarrow$ current
- pipe diameter $\Longleftrightarrow$ film resistance

HP Memristor (S. Williams et al, 2008)

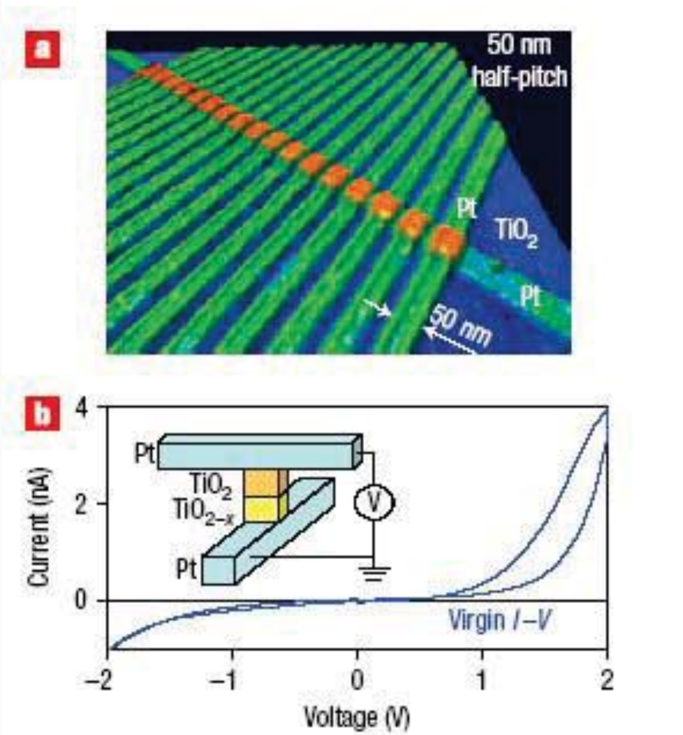

J. Yang, D. Pickett, X. Li, Ohlberg, D. Stewart, R. S. Williams, Nature Nanotech. (2008)

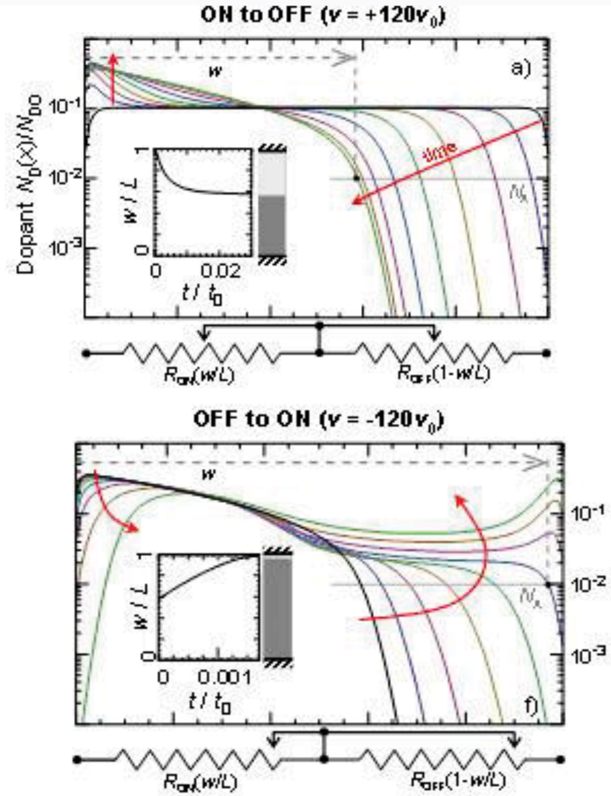

D. Strukov, J. Borghetti, R. S. Williams, Small (2008)

Electrons: $\nabla\cdot(-en(x)\,\mu_n\,\nabla\varphi_n(x)) = 0$

Holes: $\nabla\cdot(ep(x)\,\mu_p\,\nabla\varphi_p(x)) = 0$

Ions: $-\nabla\cdot(-\,eD_i\,\nabla N_D(x) - eN_D(x)\,\mu_i\,E_0\sinh[\nabla\varphi(x)/E_0]) = e\,\partial N_D(x)/\partial t$

Poisson: $-\varepsilon\varepsilon_0\Delta\varphi(x) = e[p(x)-n(x)+ f_D(x)\,N_D(x) - f_A(x)\,N_A]$

Memristor mathematical model (HP model)

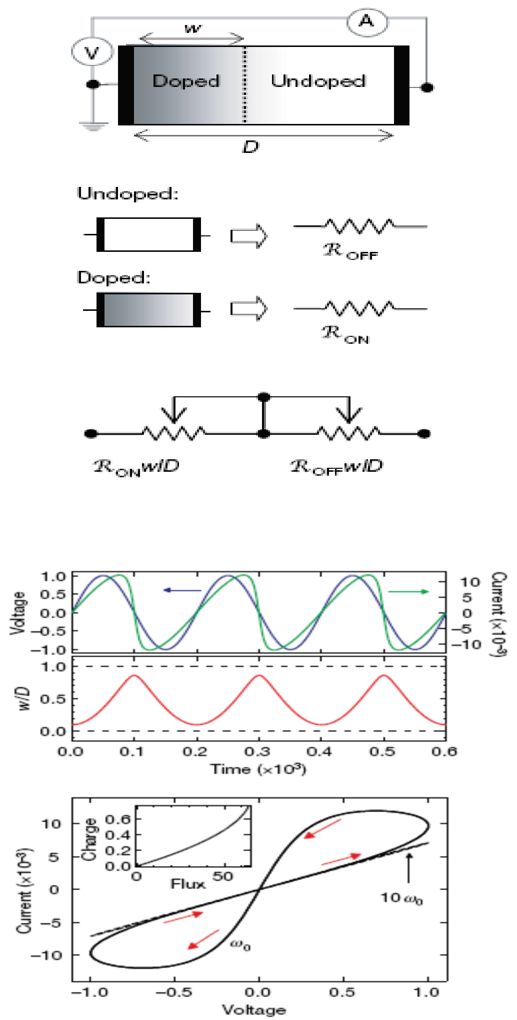

First memristor model

$$\begin{cases} \dfrac{dw(t)}{dt} = \mu \dfrac{R_{on}\frac{w(t)}{D} i(t)}{w(t)} \\ v(t) = \left(R_{on}\dfrac{w(t)}{D} + R_{off}\left(1 - \dfrac{w(t)}{D}\right)\right) i(t) \end{cases}$$

Expression for $w(t)$ as function of $q(t)$:

$$w(t) = w(t_0) + \mu \frac{R_{on}}{D}(q(t) - q(t_0))$$

For $R_{on} \ll R_{off}$ memristance expressed by

$$M(q(t)) = R_{off}\left(1 - \frac{w(t_0)}{D} - \frac{\mu R_{on}}{D^2}(q(t) - q(t_0))\right)$$

Williams et al. "The missing memristor found", *Nature*, vol. 453, pp. 80-83 2008

Memristor mathematical model

$$i(t) = W(x(t))\, v(t)$$

$$W(x(t)) = \frac{G_{on} G_{off}}{G_{on} - \Delta G x(t)}$$ memductance

with $\Delta G = G_{on} - G_{off}$, where G_{on} and G_{off} indicate the device memductance respectively in the fully-conductive and fully-insulating state (i.e. as $x(t)$ sets to 1 and 0 respectively),

$$\frac{dx(t)}{dt} = \frac{\eta}{i_0} W(x(t))\, v(t)\, F(x(t), \eta v(t), p)$$

window function

Memristor mathematical model

window function

- to account for nonlinear effects on the ionic transport ($p \in \mathbf{N}_+$ modulates the degree of such nonlinearities);
- to impose system-dependent boundary conditions.

$(a): F_J,\ p = \{1, 3, 10\}$ $(b): F_B,\ p = 2,\ \eta = 1$ $(c): \tilde{F},\ \eta = 1$

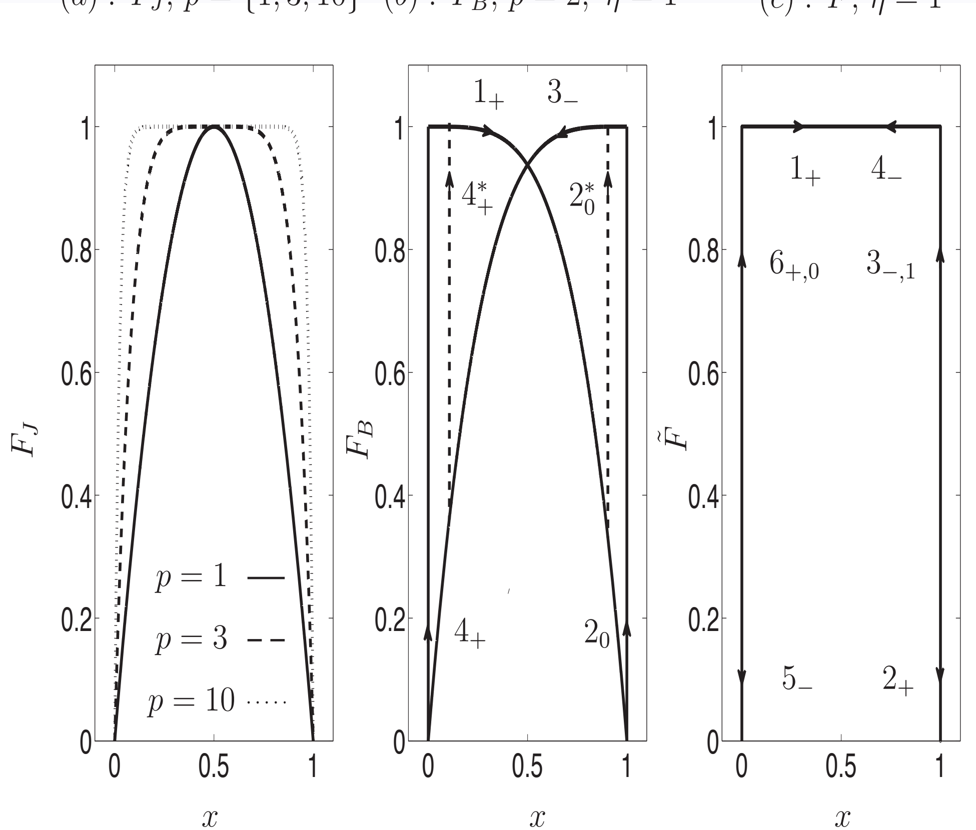

$$F_J(x, p) = 1 - (2x - 1)^{2p} \quad \forall\ \eta\, v$$

$$F_B(x, \eta\, v, p) = \begin{cases} 1 - x^{2p} & \eta\, v > 0, \\ 1 - (x-1)^{2p} & \eta\, v \leq 0. \end{cases}$$

$$F(x, v) = \begin{cases} 1 \text{ if } C_1 \text{ holds}, \\ 0 \text{ if } C_2 \text{ or } C_3 \text{ holds}. \end{cases}$$

$$\begin{aligned} C_1 &= \{\, x \in (0,1) \text{ or } (x = 0 \text{ and } v > v_{th,0}) \\ &\quad \text{or } (x = 1 \text{ and } v < -v_{th,1})\}, \\ C_2 &= \{\, x = 0 \text{ and } v \leq v_{th,0}\}, \\ C_3 &= \{\, x = 1 \text{ and } v \geq -v_{th,1}\}, \end{aligned}$$

F. Corinto and A. Ascoli, 'A boundary condition-based approach to the modeling of memristor nano-structures', IEEE Trans. on Circ. and Syst.–I, 2012, DOI: 10.1109/TCSI.2012.2190563

Memristor mathematical model
Boundary Condition-based Model (BCM)

[3] D. B. Strukov, G. S. Snider, D. R. Stewart, and R. S. Williams, "The missing memristor found," *Nature*, vol. 453, pp. 80-83, 2008.

It may be theoretically demonstrated (see Proposition 3 in [1]) that **boundary conditions may be tuned so as to obtain either single-valued or multi-valued state-flux characteristics.**

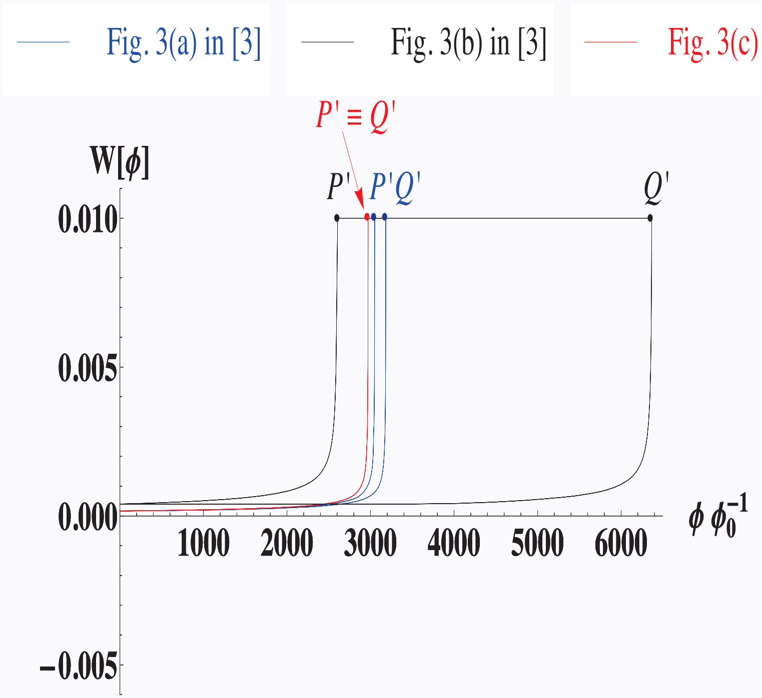

Figure 8. Memductance-flux characteristics for the memristor modeled by (1)-(2) ($x(0) = 0.1$, $G_{on} = 10^{-2}S$), using proposed window (39) and voltage source (6) with $\beta = 0.01$. Blue curve: $v_0 = 1\,V$, $G_{on}\,G_{off}^{-1} = 60$, $v_{th} = 0\,V$ (note the similarity to red curve in Fig. 4). Black curve: $v_0 = 2\,V$, $G_{on}\,G_{off}^{-1} = 25$, $v_{th} = 0\,V$. Red curve: $v_0 = 1\,V$, $G_{on}\,G_{off}^{-1} = 60$, $v_{th} = 0.5v_0\,V$ (note the similarity to red curve in Fig. 2). For each case, points $P' = (\varphi(t_{\alpha,1}), G_{on})$ and $Q' = (\varphi(t_\beta), G_{on})$ are highlighted to show whether or not one of conditions for single-valuedness, i.e. (45), is fulfilled. Here $P' \equiv Q'$ for the red curve only.

F. Corinto and A. Ascoli, 'A boundary condition-based approach to the modeling of memristor nano-structures', IEEE Trans. on Circ. and Syst.–I, 2012, DOI: 10.1109/TCSI.2012.2190563

Memristor mathematical model
Boundary Condition-based Model (BCM)

[3] D. B. Strukov, G. S. Snider, D. R. Stewart, and R. S. Williams, "The missing memristor found," *Nature*, vol. 453, pp. 80-83, 2008.

It may be theoretically demonstrated (see Proposition 3 in [1]) that **boundary conditions may be tuned so as to obtain either single-valued or multi-valued state-flux characteristics.**

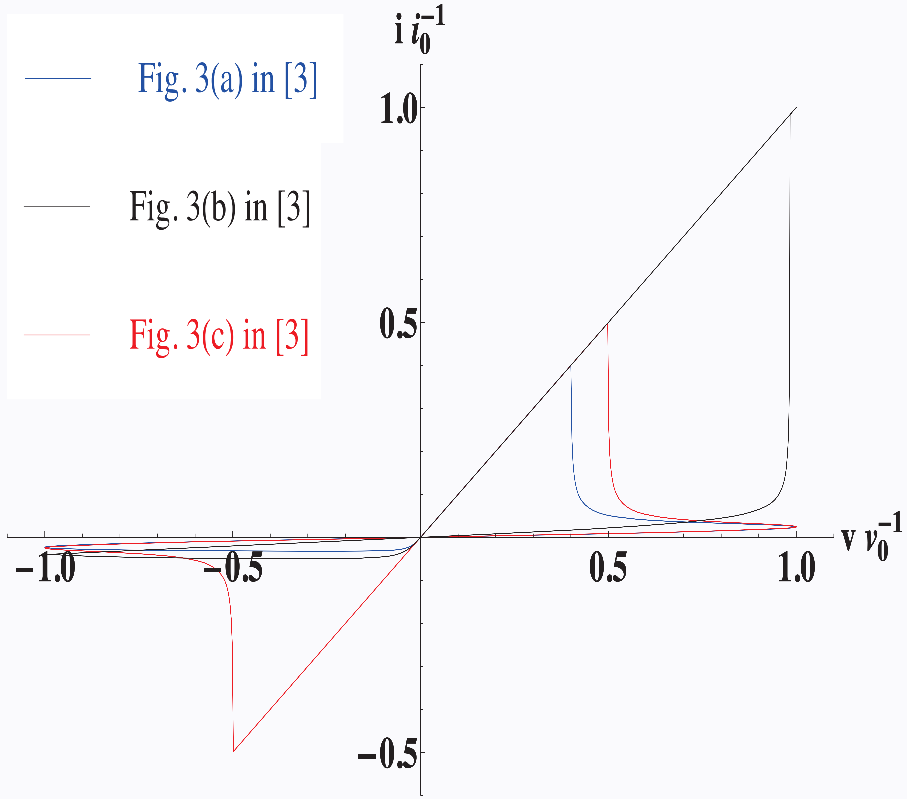

Figure 9. Current-voltage characteristics corresponding to the memductance-flux relations of Fig. 8. Blue curve is similar to red curve in Fig. 5 and to Fig. 3(a) from [3]. Black curve is similar to Fig. 3(b) from [3]. Red curve is similar to red curve in Fig. 3 and to Fig. 3(c) from [3].

F. Corinto and A. Ascoli, 'A boundary condition-based approach to the modeling of memristor nano-structures', IEEE Trans. on Circ. and Syst.–I, 2012, DOI: 10.1109/TCSI.2012.2190563

Memristor mathematical model Boundary Condition-based Model (BCM)

Table I

CAPABILITY OF EMULATION OF VARIOUS MEMRISTOR BEHAVIORS FROM [3] FOR VARIOUS MODELS PROPOSED IN LITERATURE.

Memristor $i - v$ response from [3]	Linear	Joglekar's	Biolek's	BCM
Fig. 2(b) in [3]	✓	✓	✓	Fig. 6
Fig. 2(c) in [3]	✓	✓	✓	Fig. 7
Fig. 3(a) in [3]	✗	✗	✓	Fig. 9 (blue)
Fig. 3(b) in [3]	✗	✗	✓	Fig. 9 (black)
Fig. 3(c) in [3]	✗	✓	✗	Fig. 9 (red)

BCM model captures the i – v response of other memristor nano-structures as well (see [1])

F. Corinto and A. Ascoli, 'A boundary condition-based approach to the modeling of memristor nano-structures', IEEE Trans. on Circ. and Syst.–I, 2012, DOI: 10.1109/TCSI.2012.2190563

Memristor Model Comparison

$$\frac{dw}{dt} = f_{\mathrm{off}} \sinh\left(\frac{|i|}{i_{\mathrm{off}}}\right)$$
$$\exp\left(-\exp\left(\frac{w - a_{\mathrm{off}}}{w_c} - \frac{|i|}{b}\right) - \frac{w}{w_c}\right)$$

for $i > 0$, while it is

$$\frac{dw}{dt} = -f_{\mathrm{on}} \sinh\left(\frac{|i|}{i_{\mathrm{on}}}\right)$$
$$\exp\left(-\exp\left(\frac{a_{\mathrm{on}} - w}{w_c} - \frac{|i|}{b}\right) - \frac{w}{w_c}\right)$$

second QUARTER 2013 – IEEE CIRCUITS and SYSTEMS MAGAZINE

Memristor Model Comparison

Alon Ascoli, Fernando Corinto, Vanessa Senger, and Ronald Tetzlaff

Table 4.
Comparison among the memristor models. For sake of brevity we use the acronym BM to indicate Biolek's Memristor.

	BM	BCM	Team
Test 1	-	✓	-
Test 2-a	✓	✓	✓
Test 2-b	-	-	✓
Test 2-c	✓	✓	-
Test 3	#	#	#

Figure: Test 1 aims to identify which memristor model fits better the i–v characteristic observed in the Pickett model under a particular triangular excitation. Test 2 memristor-based nonlinear circuit with periodic behavior (a) frequency of the limit cycle; b) frequency spectrum of the memristor voltage; c) transitory response due to an external pulse). Test 3 chaotic memristor-based non- linear circuit (appearance of the chaotic attractor).

Memristor modeling

Messagge to take home:
Reliable mathematical and physically-based circuit models are fundamental to develop neuromorphic hybrid systems!

Electrons: $\nabla\cdot(-en(x)\,\mu_n\,\nabla\varphi_n(x)) = 0$

Holes: $\nabla\cdot(ep(x)\,\mu_p\,\nabla\varphi_p(x)) = 0$

Ions: $-\nabla\cdot(-\,eD_i\,\nabla N_D(x) - eN_D(x)\,\mu_i\,E_0\sinh[\nabla\varphi(x)/E_0]) = e\,\partial N_D(x)/\partial t$

Poisson: $-\varepsilon\varepsilon_0\Delta\varphi(x) = e[p(x)-n(x)+ f_D(x)\,N_D(x) - f_A(x)\,N_A]$

$$v(t) = M(x,i)i$$
$$\frac{dx(t)}{dt} = f(x,i)$$
$$x(0) = x_0 \in R^n$$

Memristor modeling

and

Nonlinear dynamics

Memristor:
The role of Initial Conditions

Analysis of the memristive current-voltage behavior, i.e. make a rigorous classification of all possible current-voltage characteristics **for a sine-wave voltage-driven memristive element on the basis of amplitude, angular frequency and time history of the oscillating voltage waveform across the device**

Memristor:
The role of Initial

Appl Phys A (2011) 102: 765–783
DOI 10.1007/s00339-011-6264-9

Resistance switching memories are memristors

Leon Chua

Abstract All 2-terminal non-volatile memory devices based on *resistance switching* are *memristors*, regardless of the device material and physical operating mechanisms. They all exhibit a distinctive "fingerprint" characterized by a *pinched hysteresis loop* confined to the first and the third quadrants of the *v–i* plane whose contour shape in general changes with both the amplitude and frequency of any periodic "sine-wave-like" input voltage source, or current source. In par-

Analysis of the memr
behavior, i.e. make a
of all possible current-
for a sine-wave volta
element on the basis of amplitude, angular frequency and time history of the oscillating voltage waveform across the device

Memristor:
The role of Initial Conditions

- voltage-controlled memristor

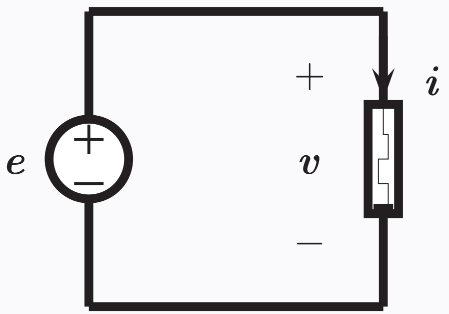

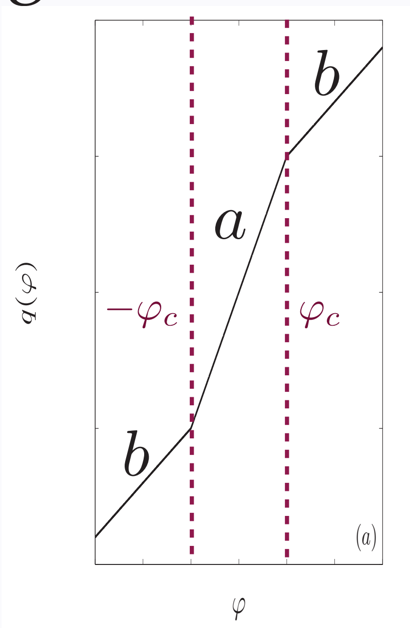

$$q(\varphi) = b\,\varphi + \frac{a-b}{2}\left(|\varphi+\varphi_c| - |\varphi-\varphi_c|\right)$$

$$a > b > 0$$

$$e(t) = E\sin(\omega t)$$

Let us set t_0=0 for simplicity.

$$\varphi(t) = \varphi(0) + \frac{E}{\omega}[1-\cos(\omega t)] = \varphi(0) + \frac{2E}{\omega}\sin^2\left(\frac{\omega t}{2}\right)$$

$$q(t) = \begin{cases} b\,\varphi(0) + \frac{2Eb}{\omega}\sin^2(\frac{\omega t}{2}) + a - b & \forall t:\ \varphi(t) \geq \varphi_c, \\ a\,\varphi(0) + \frac{2Ea}{\omega}\sin^2(\frac{\omega t}{2}) & \forall t:\ |\varphi(t)| < \varphi_c, \\ b\,\varphi(0) + \frac{2Eb}{\omega}\sin^2(\frac{\omega t}{2}) + b - a & \forall t:\ \varphi(t) \leq -\varphi_c. \end{cases}$$

$$i(t) = \begin{cases} b\,e(t) & \forall t: |\varphi(t)| \geq \varphi_c, \\ a\,e(t) & \forall t: |\varphi(t)| < \varphi_c. \end{cases}$$

$$\varphi(0) \leq \varphi(t) \leq \varphi(0) + \frac{2E}{\omega}.$$

$0 < \frac{E}{\omega} < \varphi_c$ $\qquad$ $\varphi_c \leq \frac{E}{\omega} < 2\varphi_c$ $\qquad$ $\frac{E}{\omega} \geq 2\varphi_c$

several cases by varing $\varphi(0)$

Memristor: The role of Initial Conditions

Flux initial value	Type of behavior
$\varphi(0) \geq \varphi_c$	highly-resistive behavior
$\varphi_c - \frac{E}{\omega} < \varphi(0) < \varphi_c$	atypical bow-tie with extended b-slope side and cw rotation for $v > 0$
$\varphi(0) = \varphi_c - \frac{E}{\omega}$	classical bow-tie with cw rotation for $v > 0$
$\varphi_c - \frac{2\,E}{\omega} < \varphi(0) < \varphi_c - \frac{E}{\omega}$	atypical bow-tie with extended a-slope side and cw rotation for $v > 0$
$\varphi(0) = \varphi_c - \frac{2\,E}{\omega}$	limit-subcase 1, weakly-resistive behavior
$-\varphi_c < \varphi(0) < \varphi_c - \frac{2\,E}{\omega}$	weakly-resistive behavior
$\varphi(0) = -\varphi_c$	limit-subcase 2, weakly-resistive behavior
$-\varphi_c - \frac{E}{\omega} < \varphi(0) < -\varphi_c$	atypical bow-tie with extended a-slope side and ccw rotation for $v > 0$
$\varphi(0) = -\varphi_c - \frac{E}{\omega}$	classical bow-tie with ccw rotation for $v > 0$
$-\varphi_c - \frac{2\,E}{\omega} < \varphi(0) < -\varphi_c - \frac{E}{\omega}$	atypical bow-tie with extended b-slope side and ccw rotation for $v > 0$
$\varphi(0) \leq -\varphi_c - \frac{2\,E}{\omega}$	highly-resistive behavior

Memristor:
The role of Initial Conditions

Flux initial value	Type of behavior
$\varphi(0) \geq \varphi_c$	highly-resistive behavior
$\varphi_c - \frac{E}{\omega} < \varphi(0) < \varphi_c$	
$\varphi(0) = \varphi_c - \frac{E}{\omega}$	
$\varphi_c - \frac{2\,E}{\omega} < \varphi(0) < \varphi_c - \frac{E}{\omega}$	
$\varphi(0) = \varphi_c - \frac{2\,E}{\omega}$	
$-\varphi_c < \varphi(0) < \varphi_c - \frac{2\,E}{\omega}$	
$\varphi(0) = -\varphi_c$	
$-\varphi_c - \frac{E}{\omega} < \varphi(0) < -\varphi_c$	
$\varphi(0) = -\varphi_c - \frac{E}{\omega}$	
$-\varphi_c - \frac{2\,E}{\omega} < \varphi(0) < -\varphi_c - \frac{E}{\omega}$	atypical bow-tie with extended b-slope side and ccw rotation for $v > 0$
$\varphi(0) \leq -\varphi_c - \frac{2\,E}{\omega}$	highly-resistive behavior

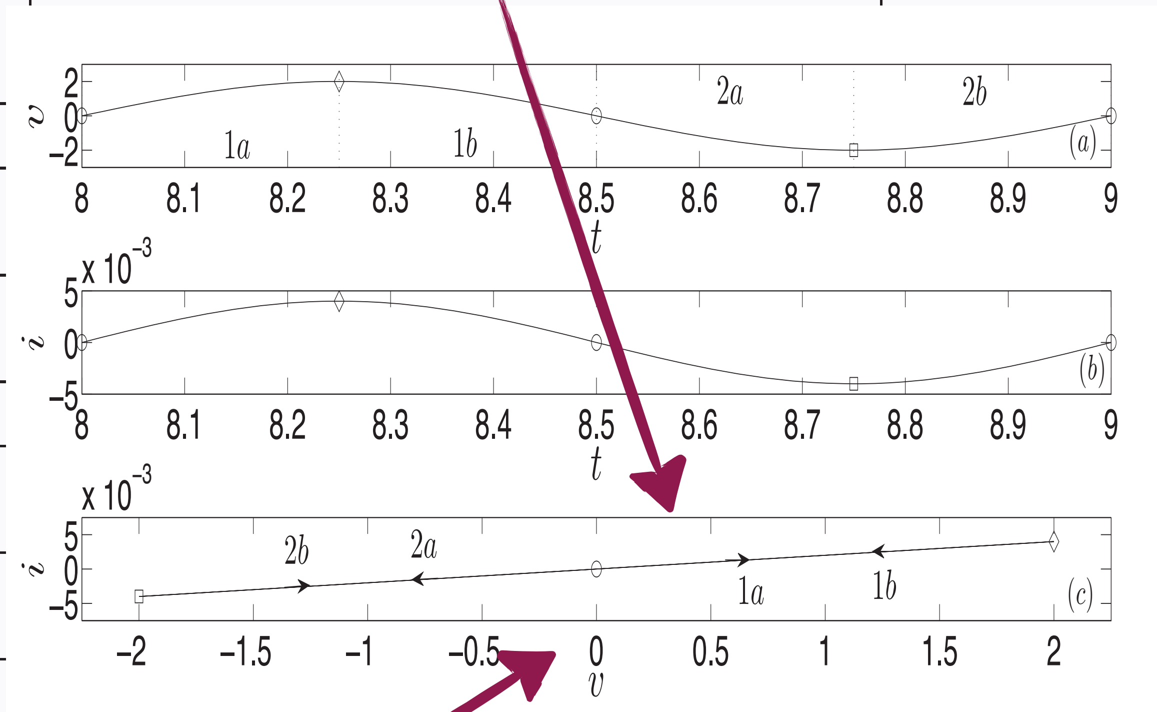

Memristor: The role of Initial Conditions

Flux initial value	Type of behavior
$\varphi(0) \geq \varphi_c$	highly-resistive behavior
$\varphi_c - \frac{E}{\omega} < \varphi(0) < \varphi_c$	atypical bow-tie with extended b-slope side and cw rotation for $v > 0$
$\varphi(0) = \varphi_c - \frac{E}{\omega}$	classical bow-tie v
$\varphi_c - \frac{2E}{\omega} < \varphi(0) < \varphi_c - \frac{E}{\omega}$	atypical bow-tie and cw rotation f
$\varphi(0) = \varphi_c - \frac{2E}{\omega}$	limit-subcase 1, w
$-\varphi_c < \varphi(0) < \varphi_c - \frac{2E}{\omega}$	weakly-resistive b
$\varphi(0) = -\varphi_c$	limit-subcase 2, w
$-\varphi_c - \frac{E}{\omega} < \varphi(0) < -\varphi_c$	atypical bow-tie and ccw rotation
$\varphi(0) = -\varphi_c - \frac{E}{\omega}$	classical bow-tie v
$-\varphi_c - \frac{2E}{\omega} < \varphi(0) < -\varphi_c - \frac{E}{\omega}$	atypical bow-tie with extended b-slope side and ccw rotation for $v > 0$
$\varphi(0) \leq -\varphi_c - \frac{2E}{\omega}$	highly-resistive behavior

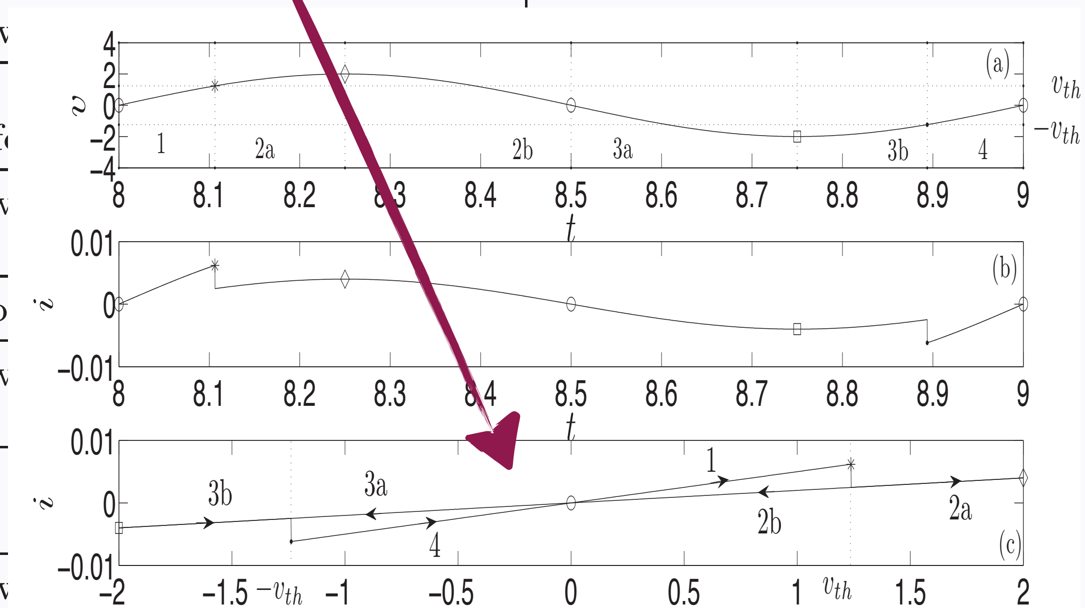

Memristor:
The role of Initial Conditions

Flux initial value	Type of behavior
$\varphi(0) \geq \varphi_c$	highly-resistive behavior
$\varphi_c - \frac{E}{\omega} < \varphi(0) < \varphi_c$	atypical bow-tie with extended b-slope side and cw rotation for $v > 0$
$-\varphi_c - \frac{2\,E}{\omega} < \varphi(0) < -\varphi_c - \frac{E}{\omega}$	atypical bow-tie with extended b-slope side and ccw rotation for $v > 0$
$\varphi(0) \leq -\varphi_c - \frac{2\,E}{\omega}$	highly-resistive behavior

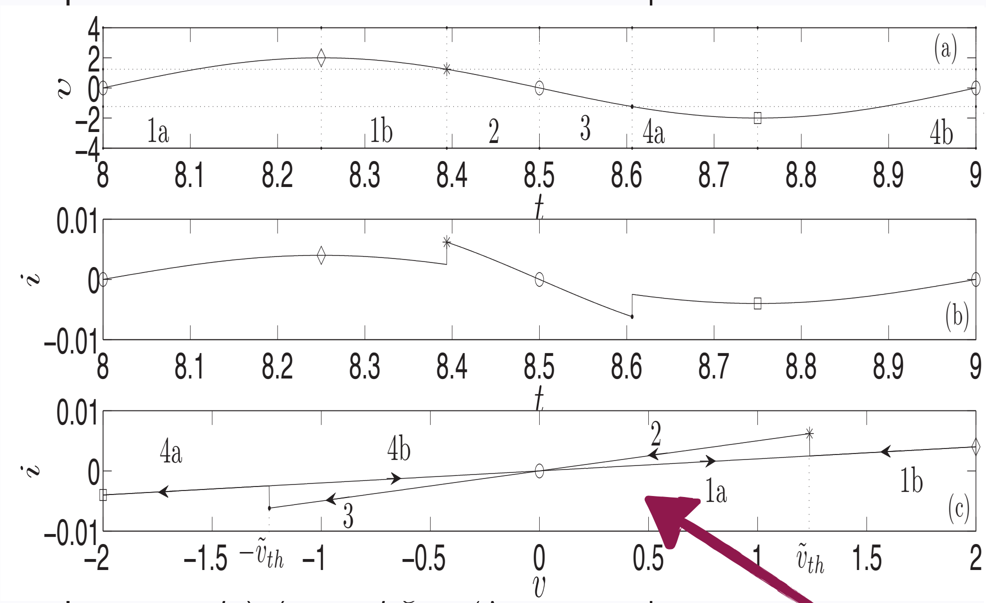

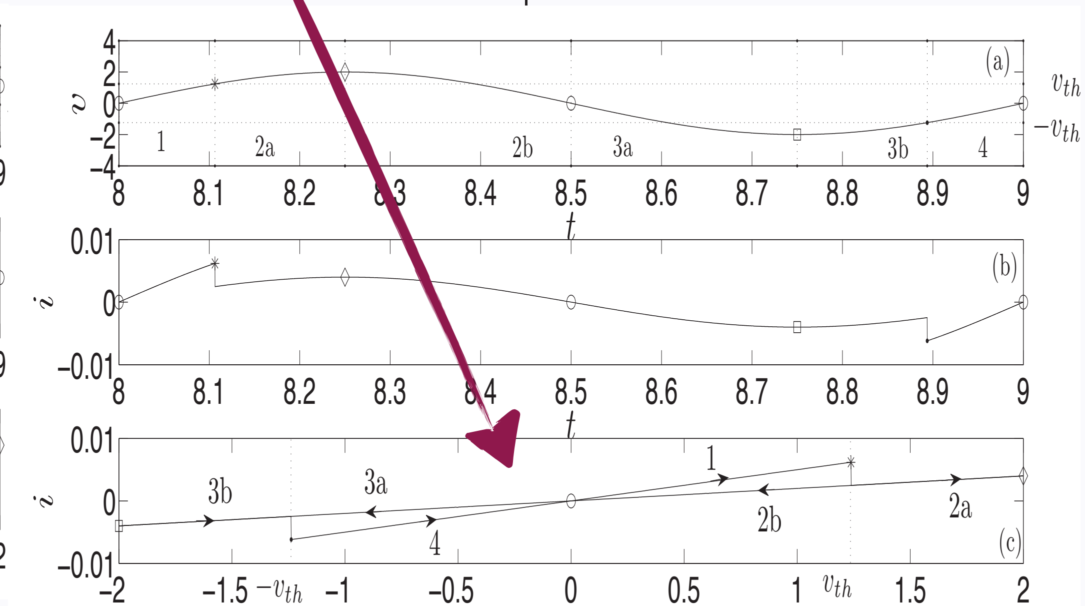

Memristor: The role of Initial Conditions

Flux initial value	Type of behavior
$\varphi(0) \geq \varphi_c$	highly-resistive behavior
$\varphi_c - \frac{E}{\omega} < \varphi(0) < \varphi_c$	atypical bow-tie with extended b-slope side and cw rotation for $v > 0$
$\varphi(0) = \varphi_c - \frac{E}{\omega}$	classical bow-tie with cw rotation for $v > 0$
$\varphi_c - \frac{2\,E}{\omega} < \varphi(0) < \varphi_c - \frac{E}{\omega}$	atypical bow-tie with extended a-slope side and cw rotation for $v > 0$
$\varphi(0) = \varphi_c - \frac{2\,E}{\omega}$	limit-subcase 1, weakly-resistive behavior
$-\varphi_c < \varphi(0) < \varphi_c - \frac{2\,E}{\omega}$	weakly-resistive behavior
$\varphi(0) = -\varphi_c$	limit-subcase 2, weakly-resistive behavior
$-\varphi_c - \frac{E}{\omega} < \varphi(0) < -\varphi_c$	atypical bow-tie with extended a-slope side and ccw rotation for $v > 0$
$\varphi(0) = -\varphi_c - \frac{E}{\omega}$	classical bow-tie with ccw rotation for $v > 0$
$-\varphi_c - \frac{2\,E}{\omega} < \varphi(0) < -\varphi_c - \frac{E}{\omega}$	atypical bow-tie with extended b-slope side and ccw rotation for $v > 0$
$\varphi(0) \leq -\varphi_c - \frac{2\,E}{\omega}$	highly-resistive behavior

Memristor:
The role of Initial Conditions

Flux initial value	Type of behavior
$\varphi(0) \geq \varphi_c$	highly-resistive behavior
$\varphi_c - \frac{E}{\omega} < \varphi(0) < \varphi_c$	atypical bow-tie with extended b-slope side and cw rotation for $v > 0$
$\varphi(0) = \varphi_c - \frac{E}{\omega}$	classical bow-tie with cw rotation for $v > 0$
$\varphi_c - \frac{2\,E}{\omega} < \varphi(0) < \varphi_c - \frac{E}{\omega}$	atypical bow-tie with e and cw rotation for $v >$ (
$\varphi(0) = \varphi_c - \frac{2\,E}{\omega}$	limit-subcase 1, weakly-r
$-\varphi_c < \varphi(0) < \varphi_c - \frac{2\,E}{\omega}$	weakly-resistive behavior
$\varphi(0) = -\varphi_c$	limit-subcase 2, weakly-r
$-\varphi_c - \frac{E}{\omega} < \varphi(0) < -\varphi_c$	atypical bow-tie with e and ccw rotation for $v >$
$\varphi(0) = -\varphi_c - \frac{E}{\omega}$	classical bow-tie with ccw rotation for $v > 0$
$-\varphi_c - \frac{2\,E}{\omega} < \varphi(0) < -\varphi_c - \frac{E}{\omega}$	atypical bow-tie with extended b-slope side and ccw rotation for $v > 0$
$\varphi(0) \leq -\varphi_c - \frac{2\,E}{\omega}$	highly-resistive behavior

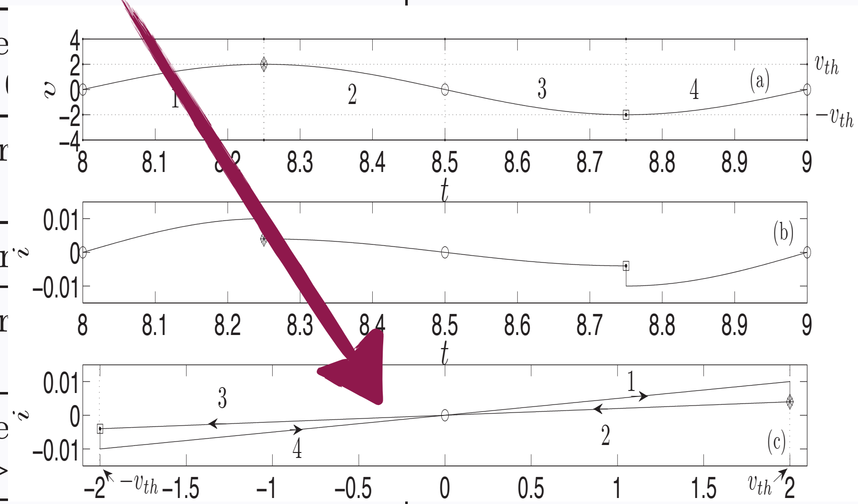

Memristor: The role of Initial Conditions

Flux initial value	Type of behavior
$\varphi(0) \geq \varphi_c$	highly-resistive behavior
$\varphi_c - \frac{E}{\omega} < \varphi(0) < \varphi_c$	atypical bow-tie with extended b-slope side and cw rotation for $v > 0$
$\varphi(0) = \varphi_c - \frac{E}{\omega}$	classical bow-tie with cw rotation for $v > 0$
$\varphi_c - \frac{2\,E}{\omega} < \varphi(0) < \varphi_c - \frac{E}{\omega}$	atypical bow-tie with extended a-slope side and cw rotation for $v > 0$
$\varphi(0) = \varphi_c - \frac{2\,E}{\omega}$	limit-subcase 1, weakly-resistive behavior
$-\varphi_c < \varphi(0) < \varphi_c - \frac{2\,E}{\omega}$	weakly-resistive behavior
$\varphi(0) = -\varphi_c$	limit-subcase 2, weakly-resistive behavior
$-\varphi_c - \frac{E}{\omega} < \varphi(0) < -\varphi_c$	atypical bow-tie with extended a-slope side and ccw rotation for $v > 0$
$\varphi(0) = -\varphi_c - \frac{E}{\omega}$	classical bow-tie with ccw rotation for $v > 0$
$-\varphi_c - \frac{2\,E}{\omega} < \varphi(0) < -\varphi_c - \frac{E}{\omega}$	atypical bow-tie with extended b-slope side and ccw rotation for $v > 0$
$\varphi(0) \leq -\varphi_c - \frac{2\,E}{\omega}$	highly-resistive behavior

Memristor:
The role of Initial Conditions

Flux initial value	Type of behavior
$\varphi(0) \geq \varphi_c$	highly-resistive behavior
$\varphi_c - \frac{E}{\omega} < \varphi(0) < \varphi_c$	atypical bow-tie with extended b-slope side and cw rotation for $v > 0$
$\varphi(0) = \varphi_c - \frac{E}{\omega}$	classical bow-tie with cw rotation for $v > 0$
$\varphi_c - \frac{2\,E}{\omega} < \varphi(0) < \varphi_c - \frac{E}{\omega}$	atypical bow-tie with extended a-slope side and cw rotation for $v > 0$
$\varphi(0) = \varphi_c - \frac{2\,E}{\omega}$	limit-subcase 1, weakly-resis
$-\varphi_c < \varphi(0) < \varphi_c - \frac{2\,E}{\omega}$	weakly-resistive behavior
$\varphi(0) = -\varphi_c$	limit-subcase 2, weakly-resis
$-\varphi_c - \frac{E}{\omega} < \varphi(0) < -\varphi_c$	atypical bow-tie with exter and ccw rotation for $v > 0$
$\varphi(0) = -\varphi_c - \frac{E}{\omega}$	classical bow-tie with ccw ro
$-\varphi_c - \frac{2\,E}{\omega} < \varphi(0) < -\varphi_c - \frac{E}{\omega}$	atypical bow-tie with exter and ccw rotation for $v > 0$
$\varphi(0) \leq -\varphi_c - \frac{2\,E}{\omega}$	highly-resistive behavior

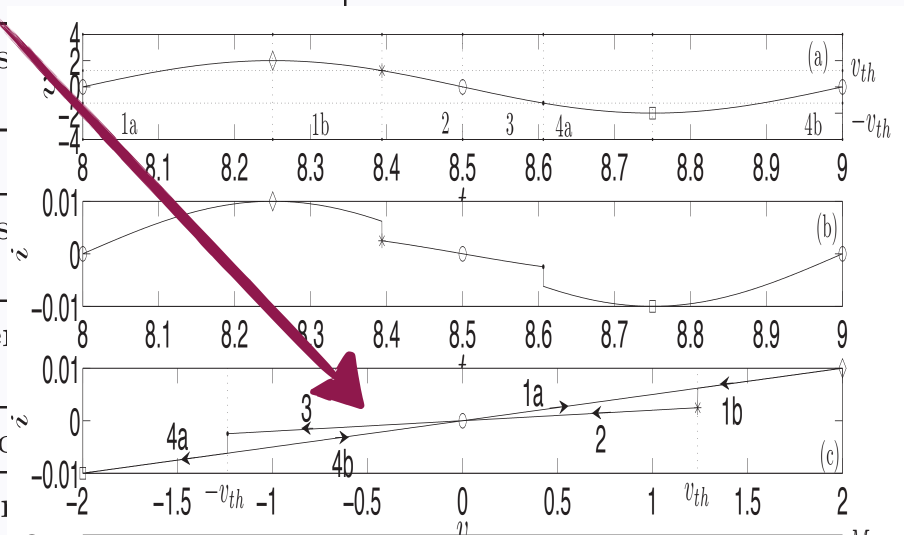

Memristor:
The role of Initial Conditions

Flux initial value	Type of behavior
$\varphi(0) \geq \varphi_c$	highly-resistive behavior
$\varphi_c - \frac{E}{\omega} < \varphi(0) < \varphi_c$	atypical bow-tie with extended b-slope side and cw rotation for $v > 0$
$\varphi(0) = \varphi_c - \frac{E}{\omega}$	classical bow-tie with cw rotation for $v > 0$
$\varphi_c - \frac{2\,E}{\omega} < \varphi(0) < \varphi_c - \frac{E}{\omega}$	atypical bow-tie with extended a-slope side and cw rotation for $v > 0$
$\varphi(0) = \varphi_c - \frac{2\,E}{\omega}$	limit-subcase 1, weakly-resistive behavior
$-\varphi_c < \varphi(0) < \varphi_c - \frac{2\,E}{\omega}$	weakly-resistive behavior
$\varphi(0) = -\varphi_c$	limit-subcase 2, weakly-resistive behavior
$-\varphi_c - \frac{E}{\omega} < \varphi(0) < -\varphi_c$	atypical bow-tie with extended a-slope side and ccw rotation for $v > 0$
$\varphi(0) = -\varphi_c - \frac{E}{\omega}$	classical bow-tie with ccw rotation for $v > 0$
$-\varphi_c - \frac{2\,E}{\omega} < \varphi(0) < -\varphi_c - \frac{E}{\omega}$	atypical bow-tie with extended b-slope side and ccw rotation for $v > 0$
$\varphi(0) \leq -\varphi_c - \frac{2\,E}{\omega}$	highly-resistive behavior

Memristor: The role of Initial Conditions

Flux initial value	Type of behavior
$\varphi(0) \geq \varphi_c$	highly-resistive behavior
$\varphi_c - \frac{E}{\omega} < \varphi(0) < \varphi_c$	atypical bow-tie with extended b-slope side and cw rotation for $v > 0$
$\varphi(0) = \varphi_c - \frac{E}{\omega}$	classical bow-tie with cw rotation for $v > 0$
$\varphi_c - \frac{2\,E}{\omega} < \varphi(0) < \varphi_c - \frac{E}{\omega}$	atypical bow-tie with extend and cw rotation for $v > 0$
$\varphi(0) = \varphi_c - \frac{2\,E}{\omega}$	limit-subcase 1, weakly-resisti
$-\varphi_c < \varphi(0) < \varphi_c - \frac{2\,E}{\omega}$	weakly-resistive behavior
$\varphi(0) = -\varphi_c$	limit-subcase 2, weakly-resisti
$-\varphi_c - \frac{E}{\omega} < \varphi(0) < -\varphi_c$	atypical bow-tie with extend and ccw rotation for $v > 0$
$\varphi(0) = -\varphi_c - \frac{E}{\omega}$	classical bow-tie with ccw rotation for $v > 0$
$-\varphi_c - \frac{2\,E}{\omega} < \varphi(0) < -\varphi_c - \frac{E}{\omega}$	atypical bow-tie with extended b-slope side and ccw rotation for $v > 0$
$\varphi(0) \leq -\varphi_c - \frac{2\,E}{\omega}$	highly-resistive behavior

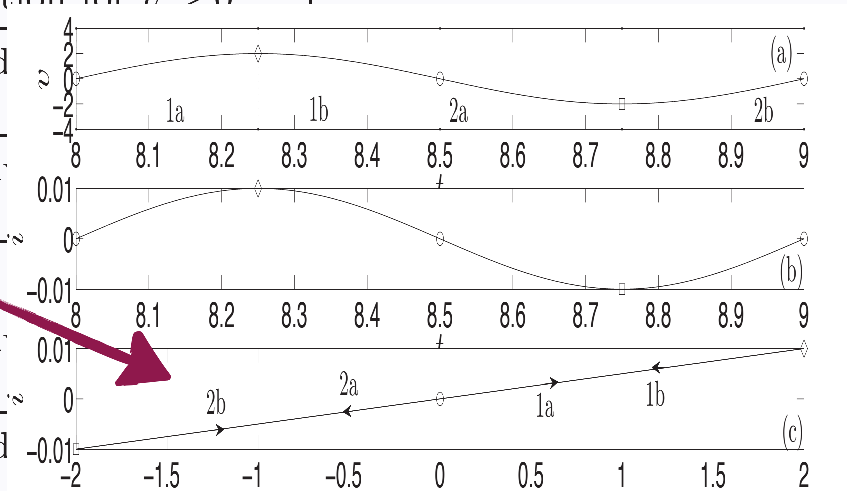

Memristor: The role of Initial Conditions

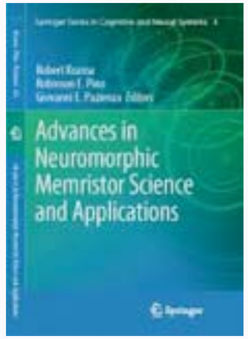

Flux initial value	Type of behavior
$\varphi(0) \geq \varphi_c$	highly-resistive behavior
$\varphi_c - \frac{E}{\omega} < \varphi(0) < \varphi_c$	atypical bow-tie with extended b-slope side and cw rotation for $v > 0$
$\varphi(0) = \varphi_c - \frac{E}{\omega}$	classical bow-tie with cw rotation for $v > 0$
$-\varphi_c < \varphi(0) < \varphi_c - \frac{E}{\omega}$	atypical bow-tie with extended a-slope side and cw rotation for $v > 0$
$\varphi(0) = -\varphi_c$	*the only limit-case for $\frac{E}{\omega} = \varphi_c$, weakly-resistive behavior*
$\varphi(0) = -\varphi_c$	limit-subcase 1 for $\frac{E}{\omega} \neq \varphi_c$, atypical bow-tie with extended a-slope side and cw rotation for $v > 0$
$-\frac{E}{\omega} < \varphi(0) < -\varphi_c$	cut atypical bow-tie with extended a-slope side and cw rotation for $v > 0$
$\varphi(0) = -\frac{E}{\omega}$	limit-subcase 2 for $\frac{E}{\omega} \neq \varphi_c$, nonlinearly-resistive behavior
$\varphi_c - 2\frac{E}{\omega} < \varphi(0) < -\frac{E}{\omega}$	cut atypical bow-tie with extended a-slope side and ccw rotation for $v > 0$
$\varphi(0) = \varphi_c - 2\frac{E}{\omega}$	limit-subcase 3 for $\frac{E}{\omega} \neq \varphi_c$, atypical bow-tie with extended a-slope side and ccw rotation for $v > 0$
$-\varphi_c - \frac{E}{\omega} < \varphi(0) < \varphi_c - 2\frac{E}{\omega}$	atypical bow-tie with extended a-slope side and ccw rotation for $v > 0$
$\varphi(0) = -\varphi_c - \frac{E}{\omega}$	classical bow-tie with ccw rotation for $v > 0$
$-\varphi_c - \frac{2E}{\omega} < \varphi(0) < -\varphi_c - \frac{E}{\omega}$	atypical bow-tie with extended b-slope side and ccw rotation for $v > 0$
$\varphi(0) \leq -\varphi_c - \frac{2E}{\omega}$	highly-resistive behavior

Flux initial value	Type of behavior
$\varphi(0) \geq \varphi_c$	highly-resistive behavior
$-\varphi_c < \varphi(0) < \varphi_c$	atypical bow-tie with extended b-slope side and cw rotation for $v > 0$
$\varphi(0) = -\varphi_c$	*limit-subcase 1 for $\frac{E}{\omega} = 2\varphi_c$, classical bow-tie with cw rotation for $v > 0$*
$-\frac{E}{\omega} = -2\varphi_c < \varphi(0) < \varphi_c - \frac{E}{\omega} = -\varphi_c$	*cut atypical bow-tie with extended a-slope side and cw rotation for $v > 0$*
$\varphi(0) = -\frac{E}{\omega} = -2\varphi_c$	*limit-subcase 2 for $\frac{E}{\omega} = 2\varphi_c$, nonlinearly-resistive behavior*
$-\varphi_c - \frac{E}{\omega} = -3\varphi_c < \varphi(0) < -\frac{E}{\omega} = -2\varphi_c$	*cut atypical bow-tie with extended a-slope side and ccw rotation for $v > 0$*
$\varphi(0) = \varphi_c - \frac{2E}{\omega} = -3\varphi_c$	*limit-subcase 3 for $\frac{E}{\omega} = 2\varphi_c$, classical bow-tie with ccw rotation for $v > 0$*
$\varphi(0) = -\varphi_c$	limit-subcase 1 for $\frac{E}{\omega} \neq 2\varphi_c$, atypical bow-tie with extended b-slope side and cw rotation for $v > 0$
$\varphi_c - \frac{E}{\omega} < \varphi(0) < -\varphi_c$	cut atypical bow-tie with extended *b*-slope side and cw rotation for $v > 0$
$\varphi(0) = \varphi_c - \frac{E}{\omega}$	cut classical bow-tie, cw rotation for $v > 0$
$-\frac{E}{\omega} < \varphi(0) < \varphi_c - \frac{E}{\omega}$	cut atypical bow-tie with extended a-slope side and cw rotation for $v > 0$
$\varphi(0) = -\frac{E}{\omega}$	limit-subcase 2 for $\frac{E}{\omega} \neq 2\varphi_c$, nonlinearly-resistive behavior
$-\varphi_c - \frac{E}{\omega} < \varphi(0) < -\frac{E}{\omega}$	cut atypical bow-tie with extended a-slope side and ccw rotation for $v > 0$
$\varphi(0) = -\varphi_c - \frac{E}{\omega}$	cut classical bow-tie with ccw rotation for $v > 0$
$\varphi_c - \frac{2E}{\omega} < \varphi(0) < -\varphi_c - \frac{E}{\omega}$	cut atypical bow-tie with extended *b*-slope side, ccw rotation for $v > 0$
$\varphi(0) = \varphi_c - \frac{2E}{\omega}$	limit-subcase 3 for $\frac{E}{\omega} \neq 2\varphi_c$, atypical bow-tie with extended *b*-slope side, ccw rotation for $v > 0$
$-\varphi_c - \frac{2E}{\omega} < \varphi(0) < \varphi_c - 2\frac{E}{\omega}$	atypical bow-tie with extended b-slope side and ccw rotation for $v > 0$
$\varphi(0) \leq -\varphi_c - \frac{2E}{\omega}$	highly-resistive behavior

F. Corinto, A. Ascoli, M. Gilli, "Analysis of Current-Voltage Characteristics for Memristive elements in Pattern Recognition Systems", Int. J. Circ. Th. and Appl. (2012)

Memristor:
The role of Initial Conditions

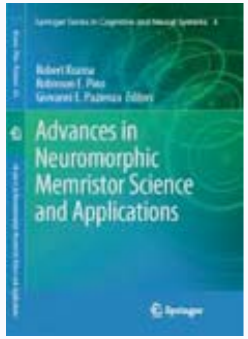

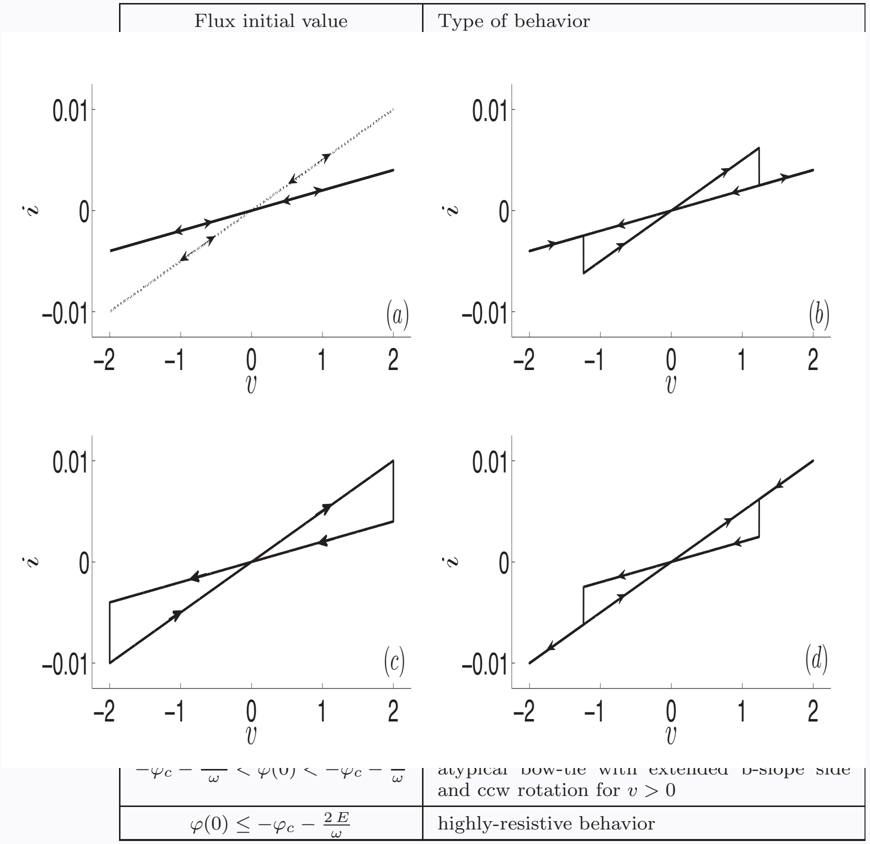

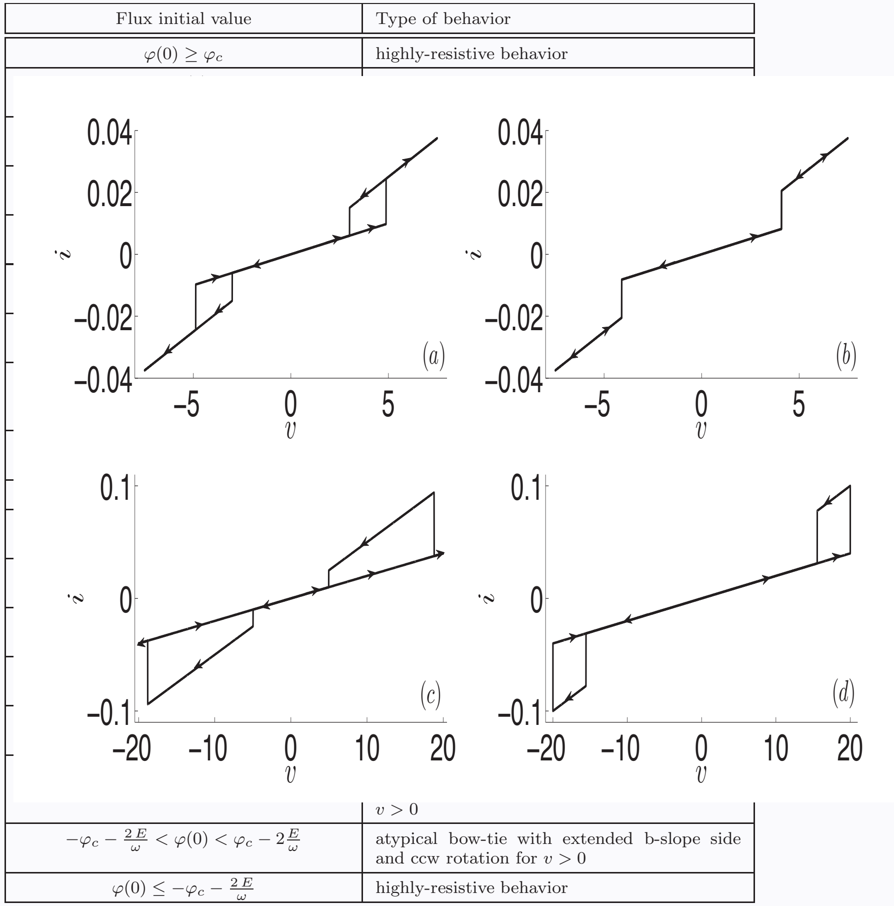

F. Corinto, A. Ascoli, M. Gilli, “Analysis of Current-Voltage Characteristics for Memristive elements in Pattern Recognition Systems”, Int. J. Circ. Th. and Appl. (2012)

Memristor:
The role of Initial Conditions

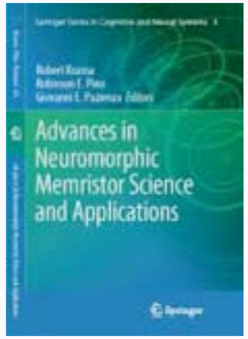

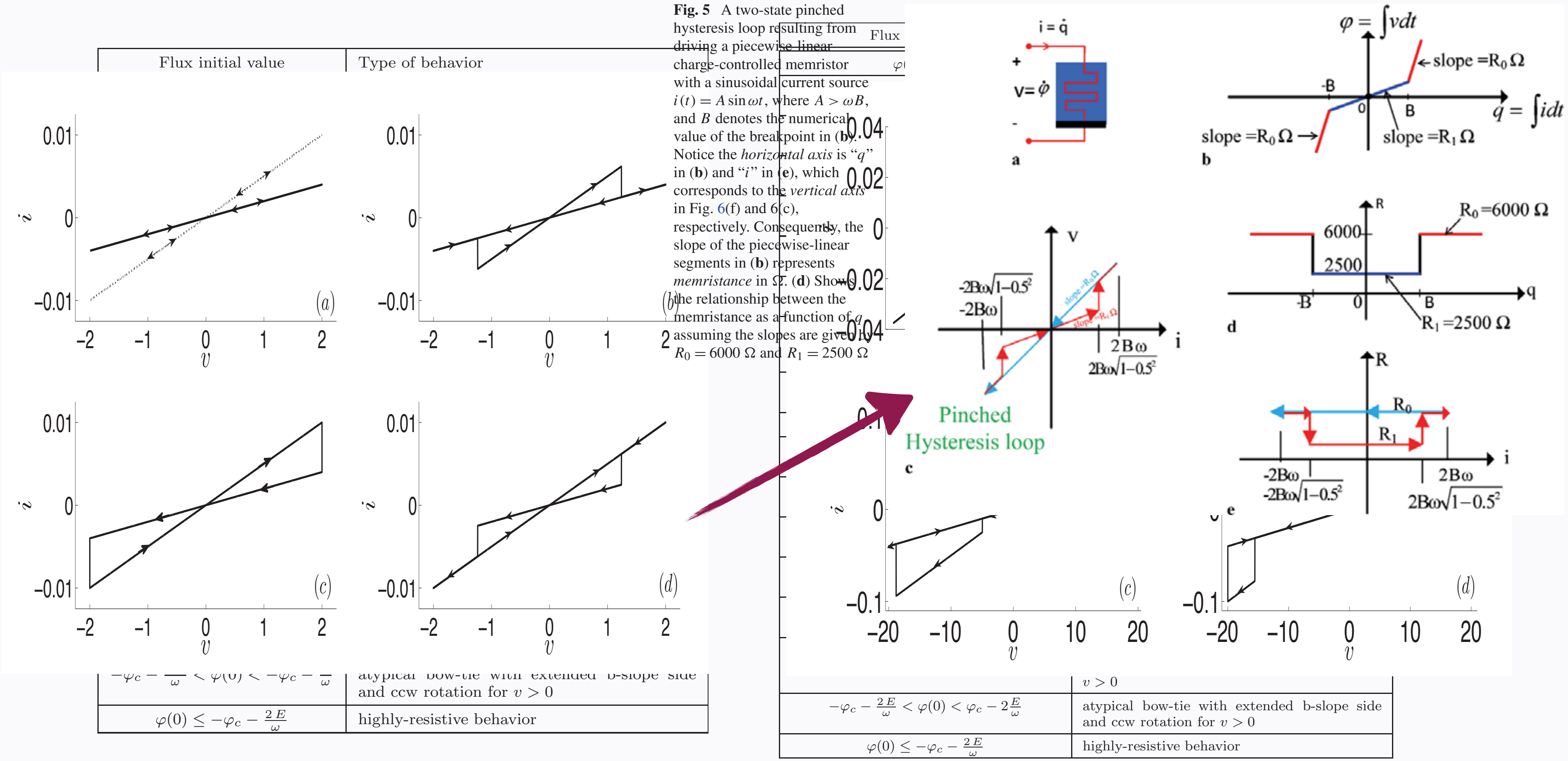

F. Corinto, A. Ascoli, M. Gilli, "Analysis of Current-Voltage Characteristics for Memristive elements in Pattern Recognition Systems", Int. J. Circ. Th. and Appl. (2012)

Memristor:
The role of Initial Conditions

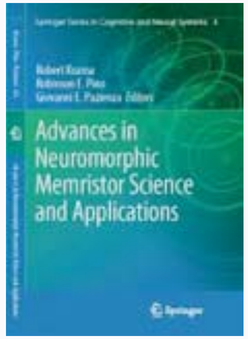

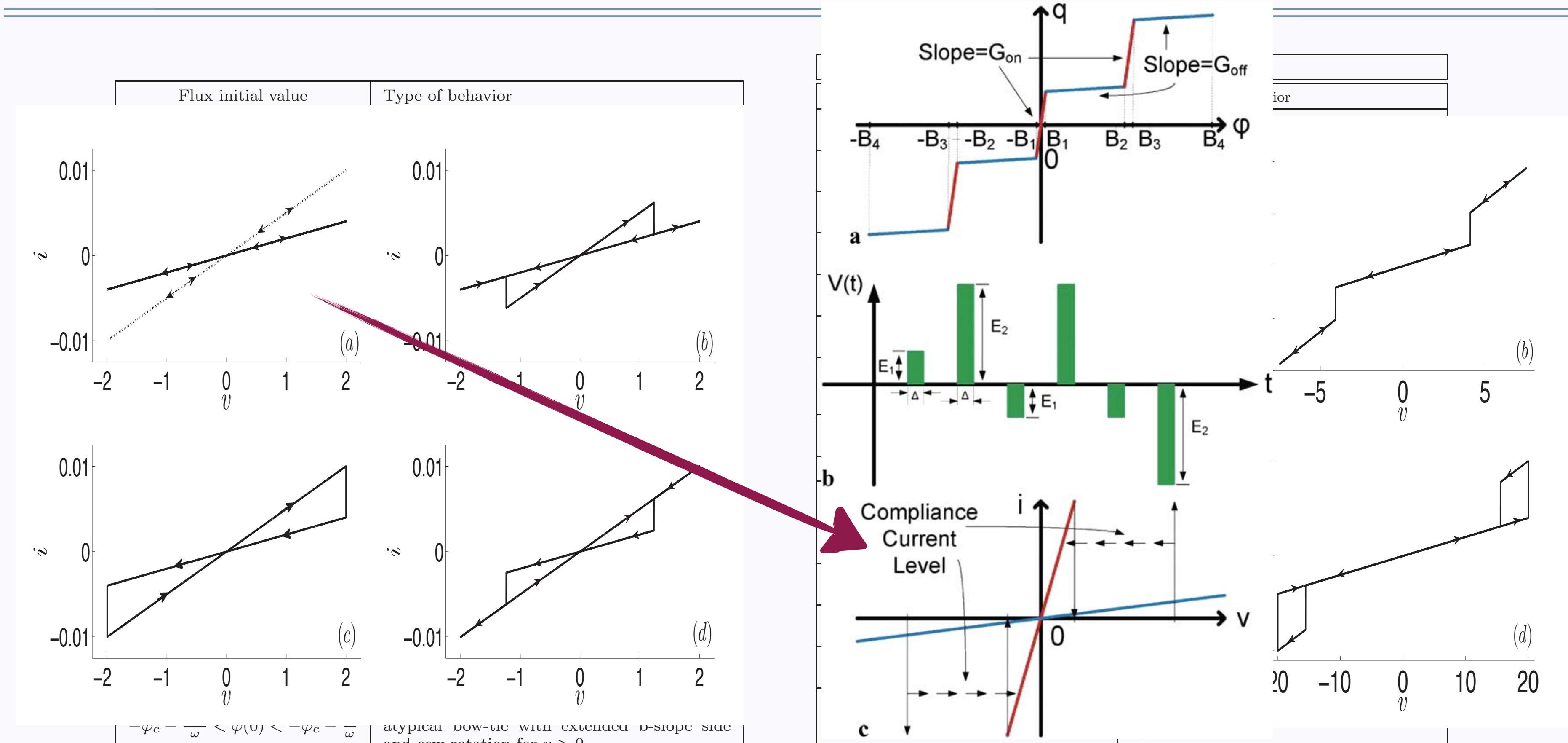

Fig. 10 A “staircase-like” flux-controlled memristor can switch from a high conductance to a low-conductance state using voltage pulses of the same polarity, somewhat reminiscent of the “unipolar” switching characteristic depicted in Fig. 1(a) of [7]

F. Corinto, A. Ascoli, M. Gilli, “Analysis of Current-Voltage Characteristics for Memristive elements in Pattern Recognition Systems”, Int. J. Circ. Th. and Appl. (2012)

Memristor: The role of Initial Conditions

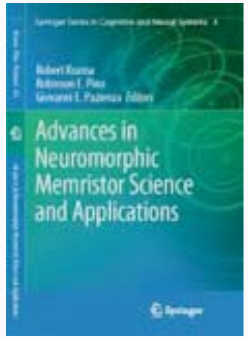

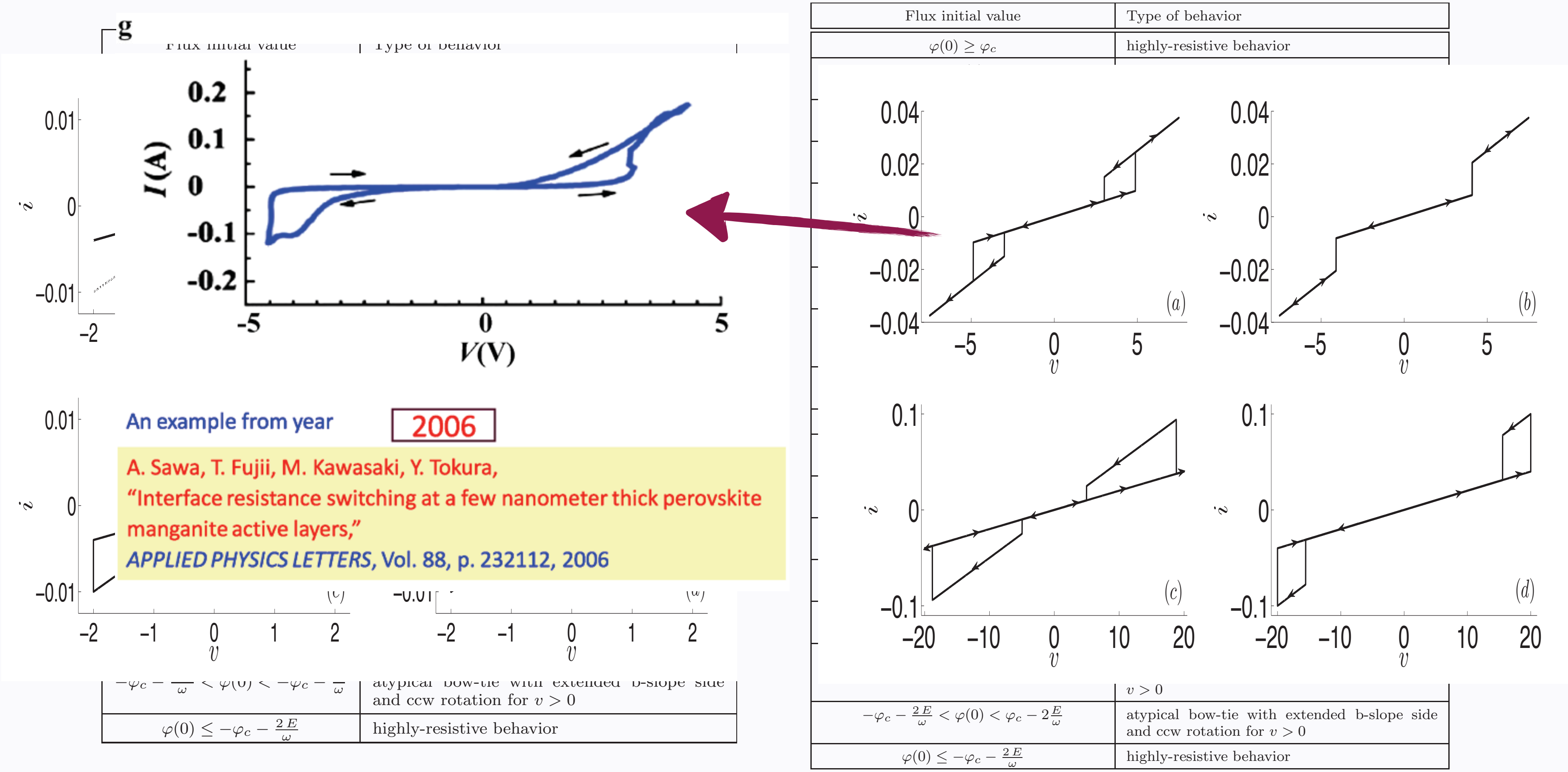

F. Corinto, A. Ascoli, M. Gilli, "Analysis of Current-Voltage Characteristics for Memristive elements in Pattern Recognition Systems", Int. J. Circ. Th. and Appl. (2012)

Memristor: The role of nonlinear dynamics

Messagge to take home:

Be carefull in applications!

The i-v curve observed in memristor devices depends on the INPUT and the INITIAL CONDITION as well.

$$v(t) = M(x,i)i$$

$$\frac{dx(t)}{dt} = f(x,i)$$

$$x(0) = x_0 \in R^n$$

Memristor oscillators

Corinto, Ascoli and Gilli "Nonlinear dynamics of memristor oscillators", IEEE Trans. on Circuits and Systems–I, vol. 58, no. 6, pp. 1323-1336, 2011

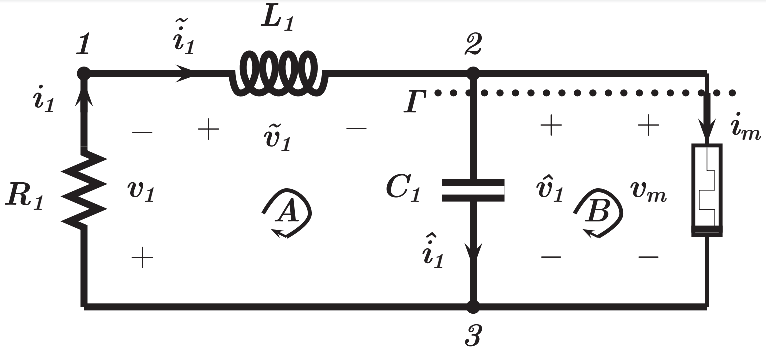

Memristor oscillator

$$i_m = W(\varphi_m)v = \frac{dq_m(\varphi_m)}{d\varphi_m}\frac{d\varphi_m}{dt}$$

$W(\varphi_m)$: **memory conductance**

With $R_1 < 0$ let

$$\alpha = C_1^{-1}, \beta = -R_1 L_1^{-1}, \xi = L_1^{-1}, \qquad x_1 = \hat{\varphi}_1, \quad x_2 = \tilde{q}_1$$

State equations are:

$$\begin{cases} \frac{d}{dt}x_1 = \alpha x_2 - \alpha q_m(x_1), \\ \frac{d}{dt}x_2 = -\xi x_1 + \beta x_2 \end{cases}$$

where

$$q_m(x_1) = bx_1 + (a-b)n(x_1), \qquad n(x_1) = \frac{1}{2}\left(|x_1+1| - |x_1-1|\right)$$

Memristor oscillators

Corinto, Ascoli and Gilli "Nonlinear dynamics of memristor oscillators", IEEE Trans. on Circuits and Systems–I, vol. 58, no. 6, pp. 1323-1336, 2011

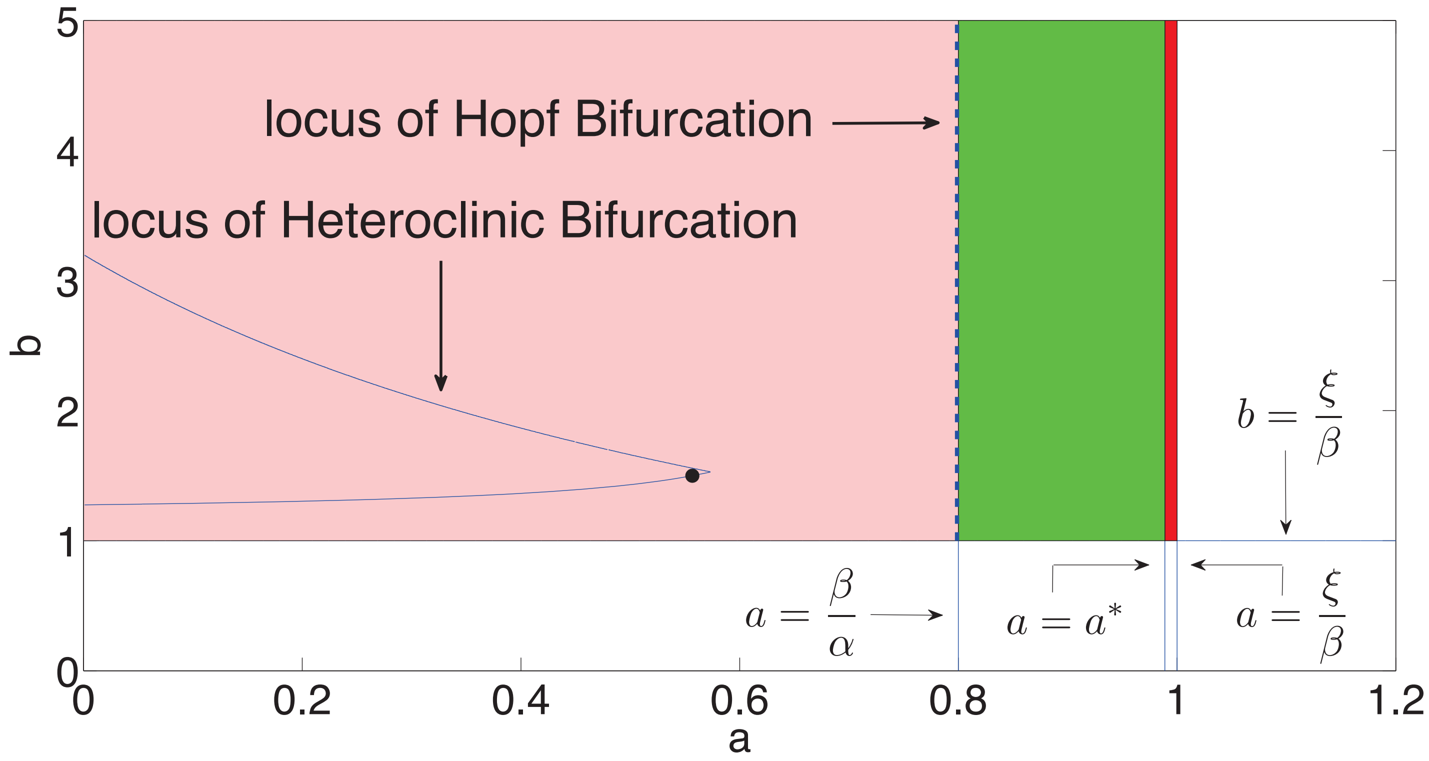

Isoline $Hb(a, b) = 0$ of the surface for $\alpha = 1.25$ and $\beta = \xi = 1$ (blue curve)

In blue: isoline point $(a, b) = (0.5568, 1.5)$

Memristor chaotic circuits

$$
\begin{aligned}
\frac{dx_1}{d\tilde{\tau}} &= -\tilde{\alpha}\left(G^{-1}(W(x_4)+W(x_5)+G_{N2})\right)x_1 - \tilde{\alpha}x_3,\\
\frac{dx_2}{d\tilde{\tau}} &= \gamma x_2 + x_3,\\
\frac{dx_3}{d\tilde{\tau}} &= \tilde{\beta}(-x_3 + x_1 - x_2),\\
\frac{dx_4}{d\tilde{\tau}} &= \frac{\eta_1}{\tilde{i}_0}W(x_4)x_1F(x_4,\eta_1W(x_4)x_1,p),\\
\frac{dx_5}{d\tilde{\tau}} &= \frac{\eta_2}{\tilde{i}_0}W(x_5)x_1F(x_5,\eta_2W(x_5)x_1,p),
\end{aligned}
$$

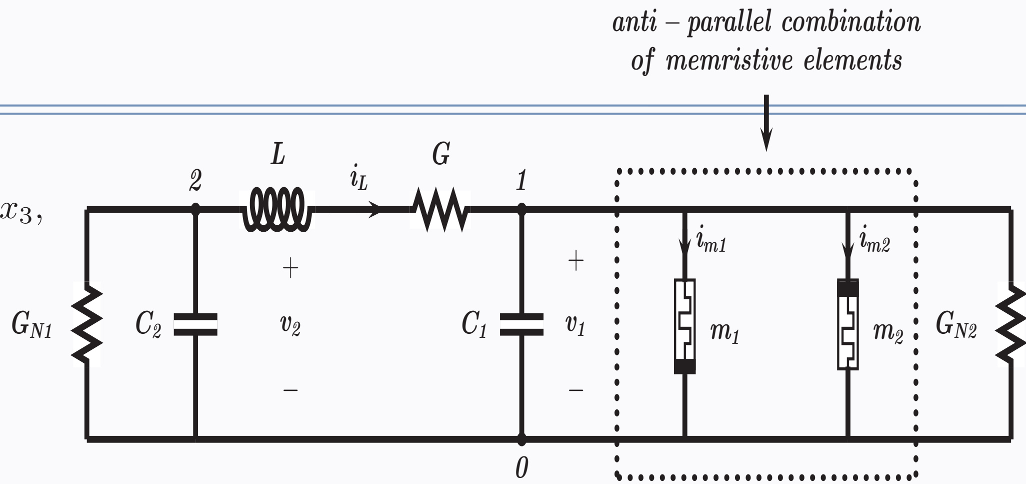

Setting circuit element values to $G = 3.3mS$, $G_{N1} = -0.4mS$, $G_{N2} = -1.2mS$, $C_1 = 50nF$, $C_2 = 37nF$ and $L = 100mH$, system parameters are numerically given by $\tilde{\alpha} = 0.74$, $\tilde{\beta} = 0.0333$ and $\gamma = 0.12$. Further $G_{off} = 0.06mS$ and $G_{on} = 1.9mS$.

$(a):\ \tilde{F},\ v_{th} = 0$ $\qquad$ $(b):\ F_B,\ p = 10$

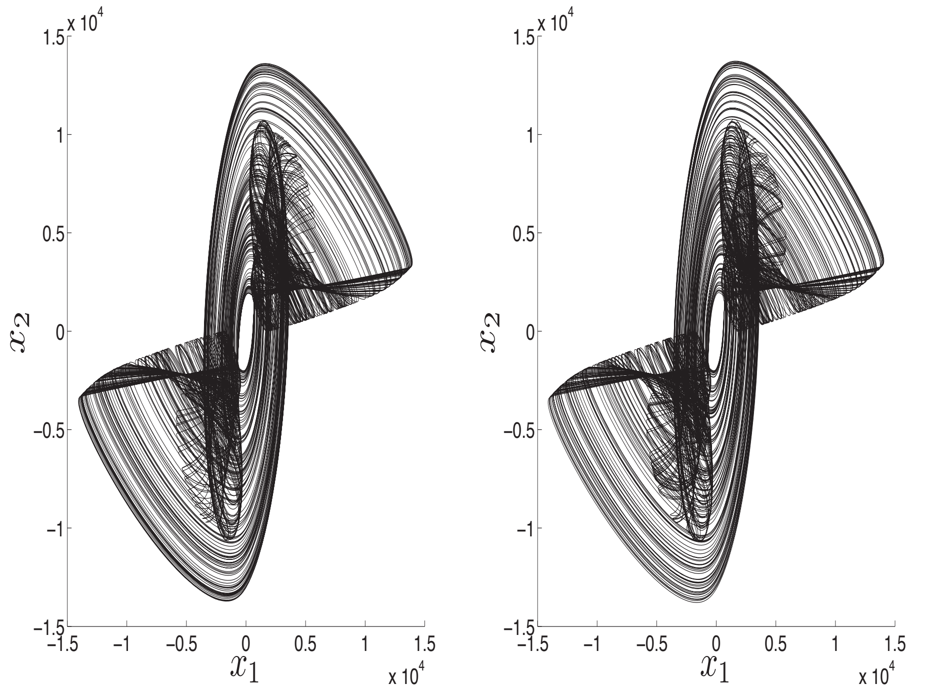

F. Corinto and A. Ascoli, 'A boundary condition-based approach to the modeling of memristor nano-structures', IEEE Trans. on Circ. and Syst.–I, 2012, DOI: 10.1109/TCSI.2012.2190563

Memristor–based Hodgkin–Huxley circuit

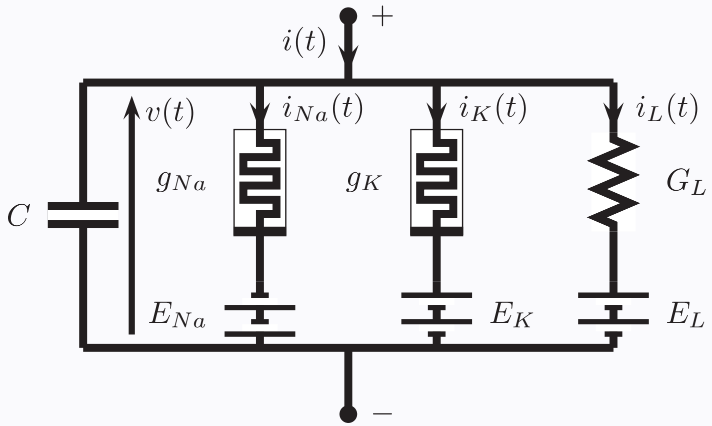

Table 3. Symbol and relevant equations defining the *Potassium Ion-Channel Memristor*.

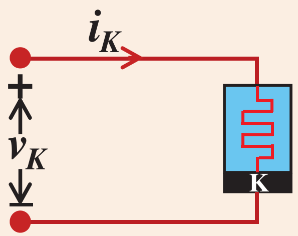

$$i_K = G_K(n)\, v_K$$

$$\frac{dn}{dt} = f_n(n, v_K)$$

$$G_K(n) \triangleq \bar{g}_K\, n^4$$

$$f_n(n, v_K) \triangleq \frac{0.01(v_K + E_K + 10)}{\exp[(v_K + E_K + 10)/10] - 1}(1-n) - 0.125 \exp\left(\frac{v_K + E_K}{80}\right) n$$

E_K=12 mV

Table 4. Symbol and relevant equations defining the *Sodium Ion-Channel Memristor*.

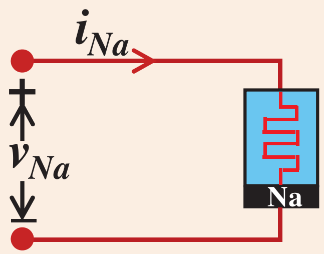

$$i_{Na} = G_{Na}(m,h)\, v_{Na}$$

$$\frac{dm}{dt} = f_m(m, v_{Na})$$

$$\frac{dh}{dt} = f_h(h, v_{Na})$$

$$G_{Na}(m,h) \triangleq \bar{g}_{Na}\, m^3 h$$

$$f_m(m, v_{Na}) \triangleq \frac{0.1(v_{Na} - E_{Na} + 25)}{\exp[(v_{Na} - E_{Na} + 25)/10] - 1}(1-m) - 4 \exp\left(\frac{v_{Na} - E_{Na}}{18}\right) m$$

$$f_h(h, v_{Na}) \triangleq 0.07 \exp\left(\frac{v_{Na} - E_{Na}}{20}\right)(1-h) - \frac{1}{\exp[(v_{Na} - E_{Na} + 30)/10] + 1} h$$

E_{Na}=115 mV

International Journal of Bifurcation and Chaos, Vol. 22, No. 3 (2012) 1230011 (48 pages)

DOI: 10.1142/S021812741230011X

HODGKIN–HUXLEY AXON IS MADE OF MEMRISTORS

LEON CHUA
VALERY SBITNEV
HYONGSUK KIM

Memristor–based Hodgkin–Huxley circuit

Memristor–based neural circuits

Fernando Corinto

Sung-Mo, "Steve" Kang

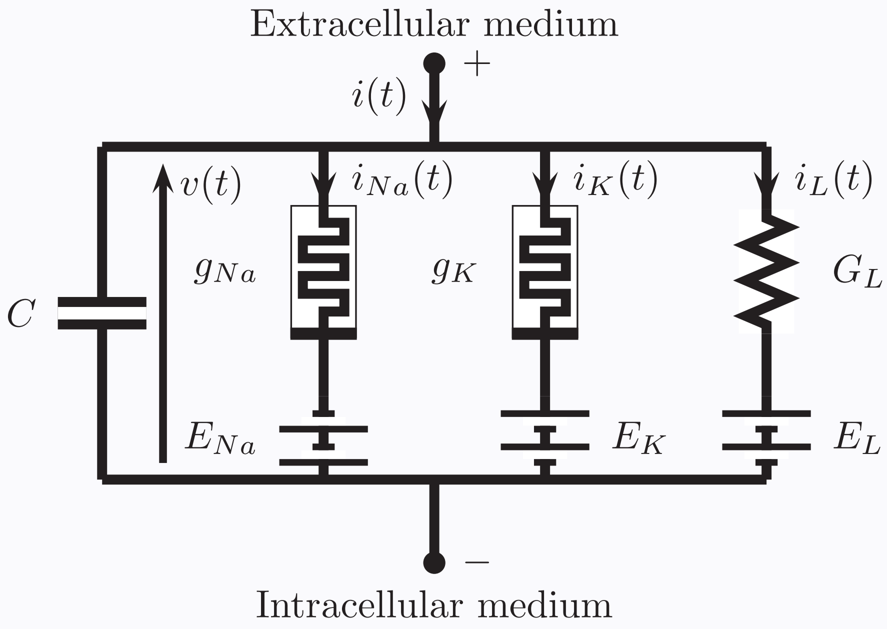

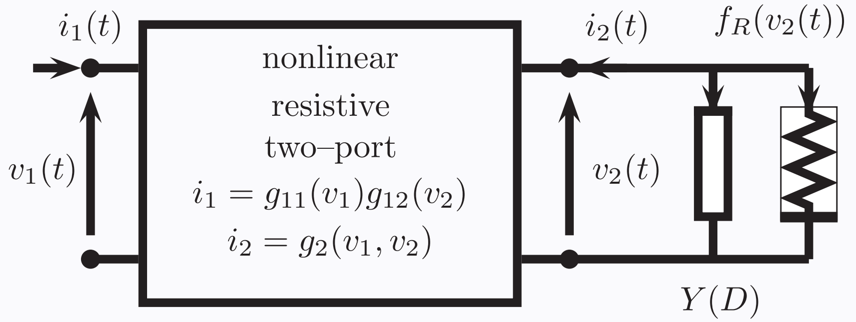

Fig. 2. Novel implementation of a memristor based on a special class of (passive) nonlinear resistive two-port connected to a nonlinear dynamic one-port.

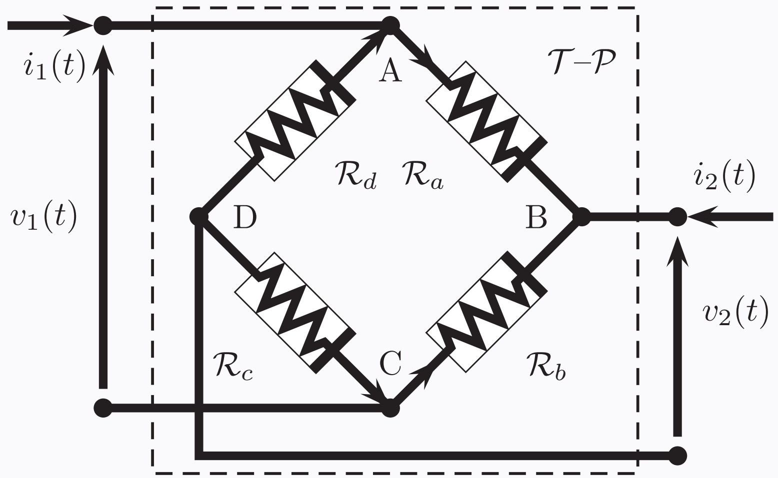

Fig. 3. Nonlinear resistive two-port connected so as to satisfy equations (5)–(7). The current in each bipole has the direction specified by the arrow and voltage is defined by the associated reference direction.

Novel circuit implementation

Memristive diode bridge with LCR filter

F. Corinto and A. Ascoli

MEMORABLE EXHIBITION

PAGE 824 Researchers in Italy have shown that a purely passive circuit, employing already-existing components, can exhibit memristive dynamics. The circuit is composed of an elementary diode bridge and an RLC series circuit, introducing nonlinearity and dynamical behaviour into the system, respectively.

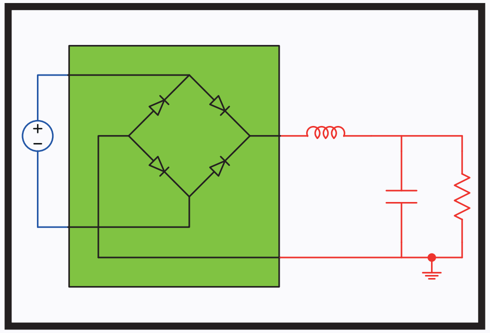

Simple electronic systems can exhibit memristive behaviour

Novel circuit implementation

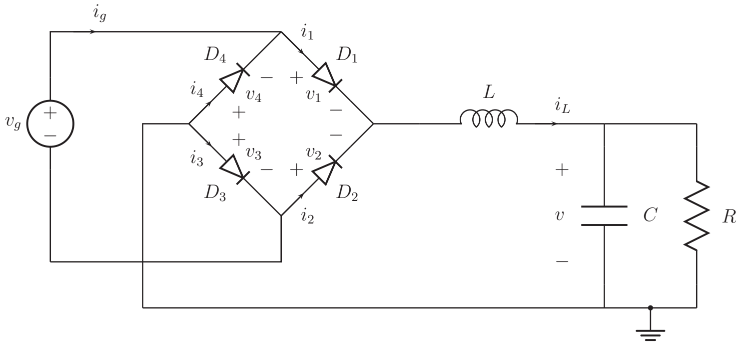

$$i_g = (i_L + 2I_S)\tanh\left(\frac{v_g}{2nV_T}\right)$$

$x_1 = v\,(V_T)^{-1}$ and $x_2 = i_L\,(I_S)^{-1}$

$$\begin{bmatrix} \beta(x_2 - \alpha x_1) \\ \gamma\left(u - x_1 - 2\ln\left(\frac{x_2+2}{2\exp(-\frac{u}{2n})\cosh(\frac{u}{2n})}\right)\right) \end{bmatrix}$$

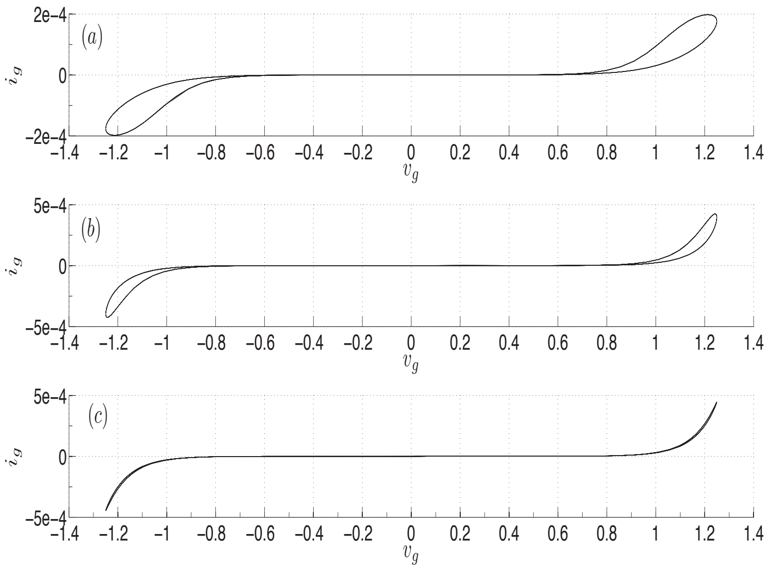

Fig. 3 *Current-voltage characteristics observed in numerical simulations of the mathematical model of the proposed circuit for a sine-wave input with f set to* 10 *(plot (a)),* 100 *(plot (b)) and* 1000 Hz *(plot (c)).*

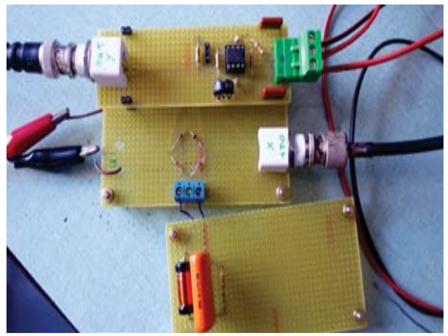

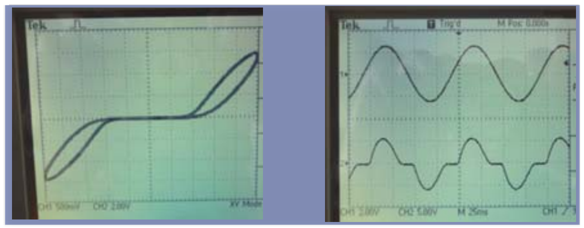

$D1N4148$, i.e. $I_S = 2.682\,nA$ and $n = 1.836$, while $V_T = 25\,mV$

$R = 1.5K\Omega \quad C = 4\mu F$ and $L = 2.5\mu H$

Potassium-Ion Channel memristor emulator

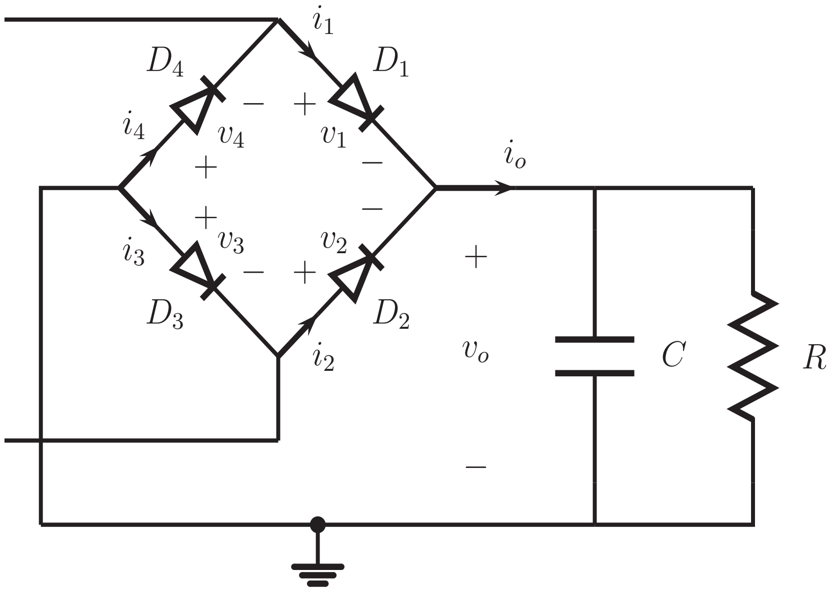

Figure: First–order voltage–controlled memristor emulator.

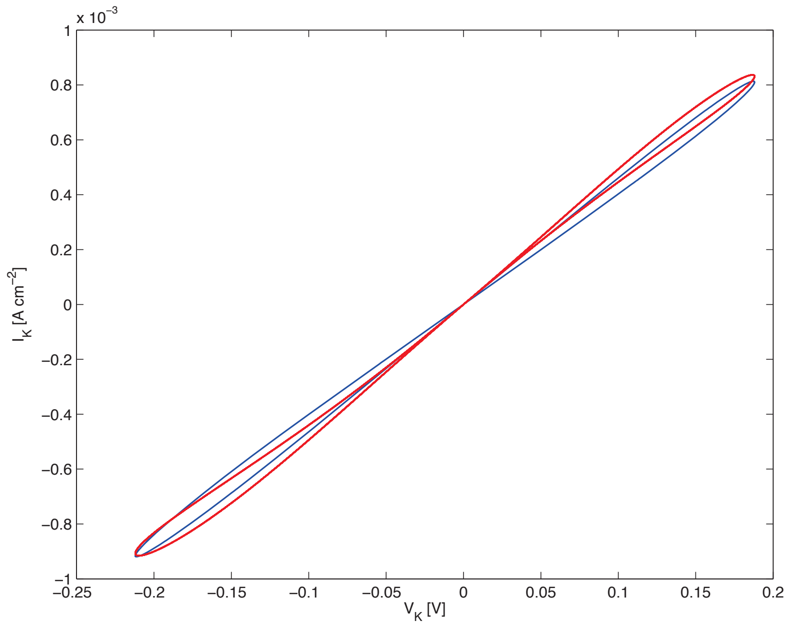

Figure: $i(t)$–$v(t)$ curve of an individual potassium channel with sinusoidal input. The red curve is obtained by integrating the HH equations, while the blue curve is the output from the PSpice implementation of the memristor circuit.

Perspectives

Memristor circuit modeling and
nonlinear dynamics in
hybrid neuromorphic circuit with
memristor-based computing nanoscale device.

↓

Unconventional Computing Systems

Conclusion

Thanks to:

- The Ministry of Foreign Affairs ”Con il contributo del Ministero degli Affari Esteri, Direzione Generale per la Promozione del Sistema Paese”
- A. Ascoli, S. Kang, K-S. Min, V. Senger, R. Tetzlaff

References (selected pubblications - see complete list at http://personal.delen.polito.it/Fernando.Corinto/):

[1] A. Ascoli, F. Corinto, V. Senger, and R. Tetzlaff “Memristor Model Comparison”,IEEE Circuits and Systems Magazine, vol. 13, no. 2, pp. 89–105, DOI: 10.1109/MCAS.2013.2256272, 2013

[2] F. Corinto, A. Ascoli, Memristive diode bridge with LCR filter, Electronics Letters, 5 July 2012, Volume 48, Issue 14, p.824–825 http://dx.doi.org/10.1049/el.2012.1480, 2012

[3] F. Corinto, A. Ascoli, A boundary condition-based approach to the modeling of memristor nano-structures, IEEE Trans. on Circ. and Syst.–I, DOI: 10.1109/TCSI.2012.2190563, 2012

[4] F. Corinto, A. Ascoli, and M. Gilli, “Analysis of current-voltage characteristics for memristive elements in pattern recognition systems,” Int. J. Circuit Theory Appl., DOI: 10.1002/cta.1804, 2012

[5] F. Corinto, A. Ascoli; M. Gilli, Nonlinear dynamics of memristor oscillators, IEEE TRANSACTIONS ON CIRCUITS AND SYSTEMS. I, REGULAR PAPERS, Vol. 58, pp. 1323-1336, ISSN: 1549- 8328, DOI: 10.1109/TCSI. 2010.2097731, 2011